Distribution Agreement

In presenting this thesis or dissertation as a partial fulfillment of the requirements for an advanced degree from Emory University, I hereby grant to Emory University and its agents the non-exclusive license to archive, make accessible, and display my thesis or dissertation in whole or in part in all forms of media, now or hereafter known, including display on the world wide web. I understand that I may select some access restrictions as part of the online submission of this thesis or dissertation. I retain all ownership rights to the copyright of the thesis or dissertation. I also retain the right to use in future works (such as articles or books) all or part of this thesis or dissertation.

Signature:

_____ _____

Mohammad Zaidi Date

Decreased Proviral DNA Loads and Changes in Innate Immune System-Related Transcription Factor Expression in Simian Immunodeficiency Virus-Infected Rhesus Macaques after Blocking the $\alpha4\beta7$ Gut-Homing Integrin

By

Mohammad Yahya Zaidi

Bachelor of Science/Master of Science

Graduate Division of Biological and Biomedical Sciences

Biology

_____
Aftab A. Ansari
Advisor

_____
Nicole M. Gerardo
Committee Member

_____
Amanda Starnes
Committee Member

_____
Darrell R. Stokes
Committee Member

Accepted:

_____
Lisa A. Tedesco, Ph.D.
Dean of the James T. Laney School of Graduate Studies

_____
Date

Decreased Proviral DNA Loads and Changes in Innate Immune System-Related Transcription Factor Expression in Simian Immunodeficiency Virus-Infected Rhesus Macaques after Blocking the $\alpha 4\beta 7$ Gut-Homing Integrin

By

Mohammad Yahya Zaidi

Advisor: Dr. Aftab A. Ansari, PhD

An abstract of

A thesis submitted to the Faculty of the James T. Laney School of Graduate Studies of Emory University in partial fulfillment of the requirements for the degree of Bachelor of Science/Master of Science in Biology

2011

Abstract

Decreased Proviral DNA Loads and Changes in Innate Immune System-Related Transcription Factor Expression in Simian Immunodeficiency Virus-Infected Rhesus Macaques after Blocking the $\alpha4\beta7$ Gut-Homing Integrin

By Mohammad Yahya Zaidi

Administration of a novel recombinant rhesus monoclonal antibody (mAb) with specificity to the $\alpha4\beta7$ gut-homing integrin prior to and 28 days after infection with the Simian Immunodeficiency Virus (SIV) resulted in a significant decrease in colorectal and jejunal proviral DNA loads of anti-$\alpha4\beta7$ treated rhesus macaques compared to control SIV-infected rhesus macaques. The anti-$\alpha4\beta7$ monoclonal antibody administration also affected innate immune system-related transcription factor expression, with significant changes in expression of the transcription factors related to Th17 cell activity and Regulatory T cell activity (Tregs) compared to the control SIV-infected rhesus macaques. Changes in innate immune system-related plasma cytokine levels were also seen in the anti-$\alpha4\beta7$ mAb treated monkeys compared to the control SIV-infected rhesus macaques. The inhibition of MIP-3α synthesis by gut tissues complemented other data collected in the lab which suggested that the anti-$\alpha4\beta7$ mAb blocks trafficking of $CD4^+$ T cells as well as inhibits the mobilization of other innate immune system cell lineages to the gut, thereby protecting the gut tissue and modulating acute SIV infection.

Decreased Proviral DNA Loads and Changes in Innate Immune System-Related Transcription Factor Expression in Simian Immunodeficiency Virus-Infected Rhesus Macaques after Blocking the $\alpha4\beta7$ Gut-Homing Integrin

By

Mohammad Yahya Zaidi

Advisor: Dr. Aftab A. Ansari, PhD

A thesis submitted to the Faculty of the James T. Laney School of Graduate Studies of Emory University in partial fulfillment of the requirements for the degree of Bachelor of Science/Master of Science in Biology

2011

Acknowledgments

This thesis would not have been possible without the continuous assistance and encouragement from my advisor, Dr. Aftab Ansari. I am truly indebted to the opportunity he has given me to participate in his research.

My entire educational career thus far would not have been possible without the unwavering support from my mother, Navida Fatima Zaidi, my father, Raza Hussain Zaidi, and my two sisters, Auj and Ailya Zaidi.

And lastly, to all my friends who never let me stop smiling, especially Ali Irfan Rae and Ilma Zejnelovic: Thank You.

Table of Contents

Introduction

A trademark of both HIV infection in humans and SIV infection in monkeys is the targeting of the virus to the gut associated lymphoid tissues (GALT) particularly, during the acute phase of infection.[i] The GALT is a mucosal barrier and one of its functions is to protect the host against the myriad of micro-organisms that can cause opportunistic infections. The GALT performs this function via the activity of a number of hematopoietic cell lineages residing within the GALT one of which are the CD4+ T cells. Due to the chronic exposure to microbiota, these CD4+ T cells are constantly activated and because of this role in protection, it normally hosts many activated $CD4^+$ T cells.[ii] The activated $CD4^+$ T cells express cell surface molecules such as the CD4 molecule and the CCR5 molecules which serve as primary receptors for HIV and SIV and thus these CD4+ T cells serve as the primary target for the HIV and SIV viruses. Infection of these cells leads to rapid virus replication and cell death and associated pathology in the gastrointestinal tissue. [iii] This pathology is thus characterized by substantial $CD4^+$ T cell depletion in the gastrointestinal tissue, chronic inflammation and immune activation with an abnormal accumulation of effector T cells in the lymph nodes, and a complete disruption of T cell homeostasis.[iv] The targeting of the GALT occurs during the acute phase which dictates that a more detailed knowledge of the step by step processes involved in gut pathology be defined. It is the present general consensus that events that occur during acute infection (extent of CD4+ T cell depletion, destruction of the epithelial cells lining the GI tissues and the rate and extent of replacement of these cells and tissues) dictate the kinetics of viral replication and the subsequent rate of disease progression.[v]

From studies detailing the early events post infection in SIV rhesus macaques, a picture of how SIV infects these monkeys can be constructed.[vi] SIV (which consists of a swarm of viruses) can cross the mucosal epithelial barrier in a matter of hours.[vii] It is now known that a

small founder population of virus appears to infect cells that expand locally during the first week of infection.[viii] This expansion produces enough infected cells in the first week of infection to establish a self-propagating systemic infection throughout the secondary lymphoid organs.[6] During the second week of infection, the SIV virus infects cells rapidly in lymphatic tissue including the GI tissues, a source of many $CD4^+$ T cells. The second and third week of infection is characterized by a peak level in virus circulating in the blood and the tissues. By the fourth to sixth week of infection, the virus levels have lowered and stabilized, and this is referred to as achieving viral load set point. However, during this process the lymphatic tissue has become a reservoir of virus and cells latently infected with provirus.[ix] It is also important to note that at this point, the SIV virus infection is not only spreading in activated, proliferating T cells, but also in resting T cells. These latently infected resting T cells are the major source of chronic infection with SIV and are the largest challenge to vaccine therapy.[8]

The early events in HIV/SIV infection must be targeted to effectively curb the rate of disease progression, and to fully understand the mechanisms involved during early infection, an understanding behind the innate immune system's role during acute infection is required.[x] This understanding includes, but is not limited to, the cell lineages present in the gastrointestinal tissue before and after HIV/SIV infection, the cytokines and cell types contributing to chronic inflammation characterized with HIV/SIV infection, and the mobilization and the kinetics of the cell lineages in response to infection.

To accomplish this goal of understanding the innate immune mechanisms of defense, it is important to understand how lymphocytes travel to the gut under physiologically normal conditions. The homing of lymphocytes from various hematopoietic sources in the body to specific skin or GI tissues has been documented, and these studies helped to establish the

science of lymphocyte trafficking.[xi] Lymphocyte trafficking is mediated by the expression of specific homing molecules on the cell surface of lymphocytes and the binding of these molecules to cognate ligands expressed by the target tissues. Generally, the homing molecules on the lymphoid cell surfaces are chemokine receptors and the target tissues that need to attract these lymphoid cells synthesize chemokines which serve as sonar wave signals to mobilize these cells to home to the target tissue and the cognate ligands where the homing molecules serve to anchor these cells to the local tissues. Specific environmental cues are obtained by the lymphocytes and induce the cells to express these homing molecules that will direct them to specific skin or gastrointestinal tissue.[xii] In the case of gut homing, vitamin A is absorbed by the gut and metabolized into retinoic acid (RA) which binds to retinoic acid receptors (RAR) expressed by lymphoid cells. Such binding of RA to RAR initiates signaling within the lymphoid cells that leads to the up regulation of the expression of the gut homing $\alpha 4\beta 7$ (a heterodimeric integrin) and CCR9 (a chemokine receptor) molecules.[xiii] Dendritic cells in the gut play a crucial role in both converting retinal to retinoic acid, and presenting retinoic acid to the appropriate retinoic acid receptors on lymphocytes.[14] The up regulated gut homing molecules $\alpha 4\beta 7$ and CCR9 on the lymphocytes bind to their cognate ligands MAdCAM and CCL25, respectively, which are expressed by endothelial and gut epithelial cells. This binding of $\alpha 4\beta 7$ and CCR9 to MAdCAM and CCL25 has been shown to effectively attract and anchor cells from the periphery and secondary lymphoid organs to the gut.[xiv] The movement of the lymphocytes from the blood via the endothelial wall and finally to the gut cells occurs through a process of adhesion of the cells to the endothelial wall, extravasation, and finally homing of the cells to the gut tissue. When the cells are moving in between the cells of the blood vessel wall, a term called diapedesis, a series of chemokine signals attract the cells to specific locations in the gut tissue.[13]

Recent findings show that not only does $\alpha4\beta7$ serve an important role in lymphocyte trafficking, but it also serves as a receptor for HIV and SIV. The HIV envelope protein gp120 binds to the $\alpha4\beta7$ integrin, which results in a rapid activation of LFA-1, an important integrin involved in cell adhesion. LFA-1 is involved in the creation of virological synapses, the main vehicle through which cell-to-cell spread of HIV occurs.[xv] This dual responsibility in facilitating progressive HIV/SIV infection highlights the importance of the $\alpha4\beta7$ integrin, compounded by the fact that most Th17 $CD4^+$ T cells express the $\alpha4\beta7$ integrin and many resting $CD4^+$ T cells express $\alpha4\beta7$, which serve as prime targets for SIV infection.[xvi] Because the GALT consists of a high frequency of $\alpha4\beta7$ expressing CD4+ T cells, their targeting is characteristic of the early, acute phase of infection. It is reasonable therefore that HIV prevention studies aim to modulate the earliest stages of infection, and the $\alpha4\beta7$ integrin serves as a logical target in preventing early viral replication and thereby curbing disease progression. Such rationale prompted the use of a novel rhesus recombinant monoclonal antibody with specificity for the $\alpha4\beta7$ integrin which was used to analyze the effects of such anti-$\alpha4\beta7$ treatment on the disease progression among SIV infected Rhesus macaques.

Hypothesis

If anti-$\alpha4\beta7$ treatment can successfully prevent $CD4^+$ T cells from traveling to the gut in SIV-infected Rhesus macaques, I predict that the pathology of the SIV infection will be dampened due to the decreased availability of potential target cells for the SIV virus during the acute phase of infection. If the anti-$\alpha4\beta7$ decreases $CD4^+$ trafficking to the gut, I predict that the pro-viral load in the anti-$\alpha4\beta7$ treated infected monkeys will be significantly less than the pro-viral loads of those infected monkeys left untreated. I also predict that the anti-$\alpha4\beta7$ treatment will lead to a significant change in expression in select transcription factors involved

in the execution of innate immune responses in the treated-infected versus untreated-infected monkeys.

Materials and Methods

Animals and administration of recombinant anti-47 monoclonal antibody:

The present study included 8 adult female rhesus macaques weighing 8 to 10 kgs housed at the Yerkes National Primate Research Center of Emory University. The housing, care, diet and maintenance met the guidelines of the Committee on the Care and Use of Laboratory Animals of the Institute of Laboratory Animal Resources, National Research Council and the Department of Health and Human Services guidelines entitled "Guide for the Care and Use of Laboratory Animals". Each of the 8 animals was negative for SIV and shown to have normal baseline immune and hematological values. The animals were divided into 2 groups: 4 animals being administered the anti-$\alpha 4\beta 7$ monoclonal antibody (mAb) and the other 4 serving as controls, receiving no antibody. The rhesus recombinant monoclonal anti-$\alpha 4\beta 7$ mAb was derived from a mouse mAb and has previously shown to have specificity for the $\alpha 4\beta 7$ integrin heterodimer[xvii] and consists of rhesus IgG1 and kappa constant regions. Pharmacokinetic studies completed previously by our lab have determined that an intravenous administration of a single dose of 50 mg/kg of this anti-$\alpha 4\beta 7$mAb to adult rhesus macaques maintains plasma levels of >10 μg/ml for 28 days.[xviii] After anti-$\alpha 4\beta 7$mAb administration, there was no detectable toxicity or changes in values of standard hematological, biochemical and standard battery of kidney and liver function tests noted, and therefore the treatment was considered safe. The 4 rhesus macaques in this study therefore each received 50 mg/kg of the sterile anti-$\alpha 4\beta 7$mAb 3 days prior to SIV infection and a similar intravenous dose on day 28-post infection (pi) which were calculated to maintain a trough plasma level of > 10 ug/ml of the mAb for about 56 days post SIV infection.

Virus used for infection and mononuclear cell isolation from blood and biopsy tissues:

To determine the amount of virus to be used for infection, an endpoint dilution assay of the stock of SIV was performed to quantitatively assess the level of replication competent virus population present in the stock virus preparation. To do this, whole blood was collected from SIV negative rhesus macaques and peripheral blood mononuclear cells (PBMC) were isolated (protocol described below). The cells were depleted of their CD8+ cells and then cultured at 2 million cells /ml in a 24-well microtiter in media containing phytohemagglutin-P (PHA-P), which stimulates T cells to proliferate through indirect TCR cross-linking. Aliquots of these PHA stimulated CD8+-depleted cells were cultured in multiples in the presence of serial dilutions of the stock SIVmac239 to establish a concentration gradient of SIVmac239. The cultures were maintained for 14 days in commercially obtained RPMI-10 (Roswell Park Medium-10) culture medium supplemented with interleukin-2 (IL-2) required as a growth factor for T cells. The cultures were then analyzed to determine which dilution of the stock SIVmac239 produced 50% infected cultures versus uninfected cultures. Data analyses from these cultures were utilized to calculate the $TCID_{50}$ titer, and 200 units of this titer were used to intravenously infect each of the 8 rhesus macaques in the study on day 0. The 200 $TCID_{50}$ injection of a single lot of SIVmac239 was in a volume of 1 ml of sterile PBS (Phosphate Buffered Saline,) pH 7.4.

Mononuclear cell isolation from the blood and biopsy tissues:

Blood samples and colorectal and jejunal biopsies were collected from the monkeys before SIV infection (baseline) and at weeks 1, 2, 3, 4, 10-12 and 19-23 post infection. The blood samples were collected in two anticoagulants to prevent clotting: Ethylenediaminetetraacetic acid (EDTA) and heparin. EDTA prevents clotting by binding to calcium in the blood. The samples collected in EDTA were used for viral load determination. Heparin acts as an anticoagulant by

enhancing the specificity of antithrombin for thrombin, which inactivates thrombin, a key protein involved in blood clotting.[xix] Blood samples collected in heparin were used in this study for the determination of absolute number of hematopoietic cell lineages, pro-viral DNA loads etc. Cells isolated from the colorectal and jejunal biopsies were also used for measurement of pro-viral DNA loads and measurement of mRNA levels for transcription factors and cytokines.

To isolate the PBMCs from the blood samples received, we initially centrifuged the blood samples for 10 minutes at 2000 rpm at 25^{o}C. This initial spin separated the blood into two layers: a blood cell layer at the bottom and a plasma layer on the top. The top layer of plasma was removed and saved separately. The remaining blood cells were mixed and resuspended in 1X PBS equalized to the volume of plasma removed and to increase mononuclear cell recovery. The diluted plasma-free blood was gently layered on top of a lymphocyte separation media (Ficol-Hypaque). Both the layered blood and the heparin plasma were then centrifuged for 30 minutes at 2000 rpm at 25^{o}C. After centrifugation, the layered blood separated into four distinct layers: packed red blood cells at the bottom and a thin layer of PBMCs floating in between two layers of lymphocyte separation media. The PMBC layer was carefully removed and saved. The centrifuged plasma absent of blood cells was collected and stored at -80^{o}C. The PBMCs were then washed with 40 mL of 1X PBS for 10 minutes at 1400 rpm at 4^{o}C. The wash media was then poured off leaving the cell pellet at the bottom of the tube. The pellet was then vortexed and 10 mL of RPMI-10 were added. The cells were either utilized immediately (fresh) or cryopreserved in freezing media (RPMI-10 with 7.5 % dimethyl sulfoxide which serves as a cryoprotectant to prevent freezing damage to the cells) and stored in liquid nitrogen.

To isolate the intraepithelial lymphocytes (IEL) and the lamina propia lymphocytes from the gut biopsies, 1.5 to 3 inches of the gut tissue were placed in 10 mL of RPMI-10. The tissue

was scraped to remove excess mucus and the tissue washed with media was aspirated twice. The tissue was then centrifuged and resuspended in PBS. Collagenase solution was added and incubated with the tissue for 2 hours to break the peptide bonds in the collagen. The exuding cell suspension was then passed through a 21G needle several times and strained twice through a 100μM and 40 μM strainer. The 40 μM separated cells were then centrifuged and resuspended in RPMI-10F and overlayed onto 60% Percoll gradient solution. The gradient was centrifuged, aspirated on 30% Percoll solution, and the cells were collected at the interface of the 30%/60% Percoll solutions. The cells were then aspirated, mixed with RPMI-10F, centrifuged, resuspended again in RPMI-10F and counted.

Isolation of Cellular DNA:

Total genomic DNA was isolated from the PBMC, colorectal, and jejunal cells using the Qiagen DNeasy kit (Qiagen, Valencia, CA). A maximum of 5×10^6 cells were thawed and centrifuged for 5 minutes at 300 rpm. The cell pellet was resuspended in 200 μL of PBS and 20 μL of proteinase K was added to degrade the proteins present in the cell samples. 4 μL of RNase A was also added to ensure RNA-free genomic DNA. 200 μL of Buffer AL (a lysis buffer) was then added and incubated with the sample at 56^oC for 10 minutes. 200 μL of ethanol was then added to the sample and mixed. The entire sample was then added to a DNeasy Mini spin column and placed in a collection tube and centrifuged at 8000 rpm for 1 minute. The spin column was then placed in a new collection tube and 500 μL of Buffer AW1 (a wash buffer) was added and the sample was centrifuged once more at 8000 rpm for 1 minute. The spin column was placed again in a new collection tube and 500 μL of Buffer AW2 (a wash buffer) was added and centrifuged for 3 minutes at 14000 rpm to dry the DNeasy membrane of the spin column. The spin column was placed again in a new collection tube and 200 μL of nuclease free water was added directly on the DNeasy membrane and incubated at room temperature for 1 minute. This was then

centrifuged for 1 minute at 8000 rpm to elute the DNA off the membrane into the collection tube. The concentration of the DNA in solution was determined for each sample by spectrometry. 4 μl of the sample was diluted in 96 μl of nuclease free water. An aliquot of the sample was placed in a spectrophotometer and the optical density at 260 nm of light was determined that served to define the concentration of DNA in the sample. The samples were ensured to have [the optical density at 260 nm/ the optical density at 280nm] be between 1.8 and 2.0 to ensure pure preparations of DNA.

Calculation of the Pro-viral Load in PBMC, colorectal and jejunal cells:

To calculate the pro-viral load in the PBMC, colorectal, and jejunal cells, a real-time polymerase chain reaction (PCR) was conducted to amplify and quantify the SIV gag gene, a gene responsible for coding viral core proteins, which had reverse transcribed into the macaque genome. The reaction used a SYBR® Green PCR Master Mix from Applied Biosytems by Life Technologies (Life Technologies, Carlsbad, California) which contained SYBR Green 1 Dye that preferentially binds to double stranded DNA, a heat stable DNA polymerase, dNTPs with dUTP and buffers optimized for the PCR. The primer pair specific for SIV gag for the pro-viral load determination was: forward (5'- GCAGAGGAGGAAATTACCCAGTAC-3') and reverse (5'-CAATTTTACCCAGGCATTTAATGTT-3'). The reaction used 10 μL of the SYBR green master mix, 1 μL of the forward primer, 1 μL of the reverse primer, 1 μL of the isolated DNA, and 7 μL of nuclease free water. DNA extracted from a fixed number of the SIV1C cell line, which has one copy of SIV DNA per cell, was used as a control for the quantization of pro-viral DNA. The PCR determined values were used to quantify the number of viral copies and expressed as number of copies per nanogram of DNA extracted from the mononuclear cells.

Isolation of Cellular RNA and Reverse Transcription of RNA:

Total RNA was isolated from the PBMC, colorectal, and jejunal cells using the Qiagen RNeasy kit (Qiagen, Valencia, CA). A maximum of 5 x 10^6 cells were thawed and 350 μL of Buffer RLT (a lysis buffer) was added. The lysate was homogenized by vortexing for 1 minute. 350 μL of 70% ethanol was then added and mixed. The mixed sample was then added to an RNeasy spin column placed in a collection tube and centrifuged for 15 seconds at 10000 rpm. 700 μL of Buffer RW1 (a wash buffer) was then added to the spin column and centrifuged for 15 seconds at 10000 rpm. 500 μL of Buffer RPE was then added to the spin column and centrifuged at 10000 rpm for 15 seconds to wash the membrane. 500 μL of Buffer RPE was then added again and centrifuged for 2 minutes at 10000 rpm to wash the spin column membrane. The spin column was then placed in a new collection tube and 50 μL of RNase free water was added directly to the spin column membrane, and this was centrifuged for 1 minute at 8000 rpm to elute the RNA. The concentration of RNA was determined using the same method used to determine the concentration of DNA as described above.

To reverse transcribe the RNA into cDNA, a reverse transcription reaction was conducted on the RNA samples using the Sigma Enhanced Avian RT First Strand Synthesis Kit (Sigma, St. Louis, Missouri). 5 μl of the RNA template (concentration between .005-.25 μg/μl) was added on ice to 1 ml of deoxynucleotide mix, 1 μL of oligo $(dT)_{23}$ and 3μl of water. This was mixed and briefly centrifuged. The solution was then placed in a thermal cycler at 70°C for 10 minutes. The tube was then placed on ice and 2 μL of 10X buffer for eAMV-RT, 1 μL of enhanced avian RT, 1 μL of RNase inhibitor, and 6 μL of nuclease free water were added. This was then placed in a thermal cycler at 50°C for 50 minutes. After this incubation was complete, the cDNA was formed and the concentration was determined using the spectrometry methods described above.

Quantitative mRNA analysis:

To calculate the relative levels of messenger RNA (mRNA) coding for a select number of transcription factors deemed to be of interest in the colorectal mononuclear cells, a real time PCR was conducted using the Taqman primer pairs and probe and the 96-well assay system (Applied Biosystems, Step One plus real time PCR Assay, Carslbad, CA). The primer pairs and probe used to identify the transcription factors were either specific for rhesus macaques or human reagents that were known to cross-react with rhesus macaque samples. The Applied Biosystem kits use the rhesus beta-2-microglobulin as the reference value, in that β2-microglobulin has a constant value of expression within the cell. The TaqMan® assays used a Gene Expression Master Mix from Applied Biosystems which included a DNA polymerase and buffers to optimize PCR efficiency. Each sample was run with 10 μL of the Gene Expression Master Mix, 1 μL of the Taqman Assay Mix which included the primer pairs specific for the target transcription factor, 1 μL of the isolated cDNA, and 8 μL of nuclease free water. Software provided by the manufacturer was used to calculate the values of the ΔΔCT for the samples. The cycle threshold (CT) values in the real-time PCR are the number of cycles required for the florescent signal from the DNA amplification to cross a certain threshold and are inversely proportional to the amount of starting DNA in the samples. The ΔCT values were taken by subtracting the reference values of β2-microglobulin. The ΔΔCT values were taken by subtracting these values by the baseline values for each monkey. The transcription factors analyzed using the Taqman Assay were rhesus FoxP3, rhesus GARP, rhesus IL17A, and human ROR-Cγ. In addition to these transcription factors, the mRNA levels for rhesus IL-21, IL-22, IL-23, and MIP-3α were analyzed using the SybrGreen real time PCR assay described previously. The values of these transcription factors were expressed relative to GAPDH and the baseline values for each monkey. Table 1 identifies all the transcription factors analyzed, the manufacturer

catalog number for the primer pairs or the primer sequence, and the function of the transcription factor in the cell.

Table 1:

Transcription Factor	Sequence/ Catalog Number	Immunological Significance
β2-microglobulin	*Rh02847367-m1*	control
FOXP3	*Rh02788830-m1*	Indicator of Tregs
GARP	*Rh02916124-m1*	Indicator of Tregs
IL17A	*Rh026221759-m1*	Indicator of Th17
RORC	*Hs01076112M1*	Indicator of Th17
IL-21	*TGTGAATGACTTGGACCCTGAA and AAACAGGAAATAGCT GACCACTCA*	Influences gastro-intestinal immune interactions
IL-22	*TCCGCGGAGTCAGTATGAGTGAGC and GAACCTATCCGATTGAGGGAGC AGC*	Influences gastro-intestinal immune interactions
IL-23	*GGACAACAGTCAGTTCTGCTT and CACAGGGCTATCAGGCAGC*	Influences gastro-intestinal immune interactions
MIP-3α	*ACCATGTGCTGTACCAAGAGTTTG and CTAAACCCTCCATGATGTGCAAGTGA*	Gut chemokine involved in recruitment
GAPDH	*GCACCACCAACTGCTTAGCAC and TCTTCTGGGTGGCAGTGATG*	control

Enzyme-linked Immunosorbent Assay (ELISA) Analysis of Plasma Levels of IL-10, IL-7, IL-15, TGF-β, and IFN-α

Heparinized plasma samples were used to quantify levels of the immunological cytokines IL-10, IL-7, IL-15, TGF-β, and IFN-α. Commercial ELISA kits that were previously shown to react with Rhesus macaque proteins were used and are listed along with the immunological

significance of the cytokines measured in Table 2. Although each kit was ordered from a different manufacturer, the standard protocol for ELISA remains the same between manufacturers. The ELISA analysis used a 96 well plate pre-coated with a monoclonal capture antibody for the specific cytokine to be measured. Individual wells of these micro-titer plates were incubated with dilutions of the sample to be analyzed and after incubation for 30 min at 4°C, the plates were then washed with wash buffer (PBS/0.05% Tween 20) and incubated with a blocking buffer (PBS/ 1% Bovine Serum Albumin) to prevent non-specific binding of the capture antibody to other proteins in the plasma. For the purposes of calculating the amount of cytokine being measured in the samples, each ELISA kit came with a fixed amount of recombinant cytokine to be used in parallel. A standard dilution (ranging from 500 pg/mL to 8 pg/mL) of this cytokine was prepared from a concentrated stock solution and individual dilutions were loaded into individual wells of the 96-well plate. The plates were washed with the wash buffer to remove excess blocking buffer. The standards and plasma samples from each monkey at different time points were then loaded onto the plate and allowed to incubate for 1.5 hours. The plates were then washed using the wash buffer to remove excess plasma, and a biotinylated polyclonal secondary antibody specific for the cytokine was added to the wells and allowed to incubate for 2 hours. The plates were washed to remove excess secondary antibody, and streptavidin-conjugated horseradish peroxidase (HRP) solution was added to the wells. Streptavidin is a protein that specifically binds to biotin, and the covalently bound HRP provides enzyme activity for detection. The streptavidin-conjugated HRP solution was allowed to incubate for 1 hour, and then the wells were washed with wash buffer to remove excess solution. A substrate solution for the HRP was then added to the wells and allowed to incubate in the dark for 30 minutes. The wells turned various shades of blue once this substrate was added (darker shades of blue were seen at higher concentrations of the standard and lighter

shades were seen at lower concentrations). An acidic stop solution was then added immediately to stop the reaction of HRP and substrate. The plates were then read in a plate reader which measured the absorbance at 450 nm. The absorbance values of the standards were plotted to make a standard curve using the known concentrations. The absorbance values of the unknown plasma samples were plotted onto this standard curve to calculate the concentrations of cytokine.

Table 2:

Cytokine	Kit name	Manufacturer	Immunoligcal significance
IL-10	Quantikine® Human IL-10	R&D Systems	Immunosuppressive cytokine
IL-7	Self Made	Capture and Secondary Antibodies (R&D Systems), Streptavidin-HRP and Substrate Solutions (Biosource)	Modulator in T cell survival and T cell homeostasis
IL-15	OptEIA™ Human IL-15 ELISA Set	BD Biosciences	T Cell Growth Factor
TGF-β	TGF-β Elisa Kit	Invitrogen	Anti-inflammatory cytokine
IFN-α	Verikine™ Cynomolgus/ Rhesus IFN-a Serum ELISA Kit	PBL Interferon Source	Antiviral Cytokine

Results

Effect of in vivo anti-α4β7 mAb infusion on proviral DNA load in PBMCs and mononuclear cells from jejunal and colorectal biopsies:

The measured levels of proviral DNA in both the PBMCs and the isolated colorectal and jejunal mononuclear cells were analyzed from the monkeys that received the anti-α4β7 mAb and were compared with proviral levels from similar cells in the control monkeys. Unfractionated mononuclear samples were used in the analysis because we did not know whether the anti-α4β7 mAb administration promotes infection of other cell lineages. For the PBMC samples, low levels of proviral DNA (copies/ng DNA) were seen in the anti- α4β7 mAb treated monkeys as early as week 1 post infection (Fig. 1a). The proviral DNA levels gradually increased during week 2 (10-24 copies/ng DNA) and week 3 (8-46 copies/ ng DNA) after which levels decreased. The control animals on the other hand did not have as clear a pattern. Proviral levels in the PBMCs of control monkeys were generally lower than the levels in the anti-α4β7 monkeys (Fig. 1b). This may be a reflection of the rapid emigration of infected cells from the blood (to the gut?). Although 2 of the control monkeys showed higher proviral DNA loads in the PBMC samples at weeks 1 and 2, stable levels appeared at week 3 and decreased thereafter.

Figure 1.

Levels of proviral DNA expressed as copies per nanogram of DNA extracted from mononuclear cells from each of the four anti-α4β7 mAb-treated animals and the four control animals from whole blood samples. Proviral loads are shown individually by monkey (a) and by each experimental group (b) with the anti-a4b7 treated monkeys being the solid lines and the control groups as the broken lines. Standard error bars are shown for each group of monkeys.

a)

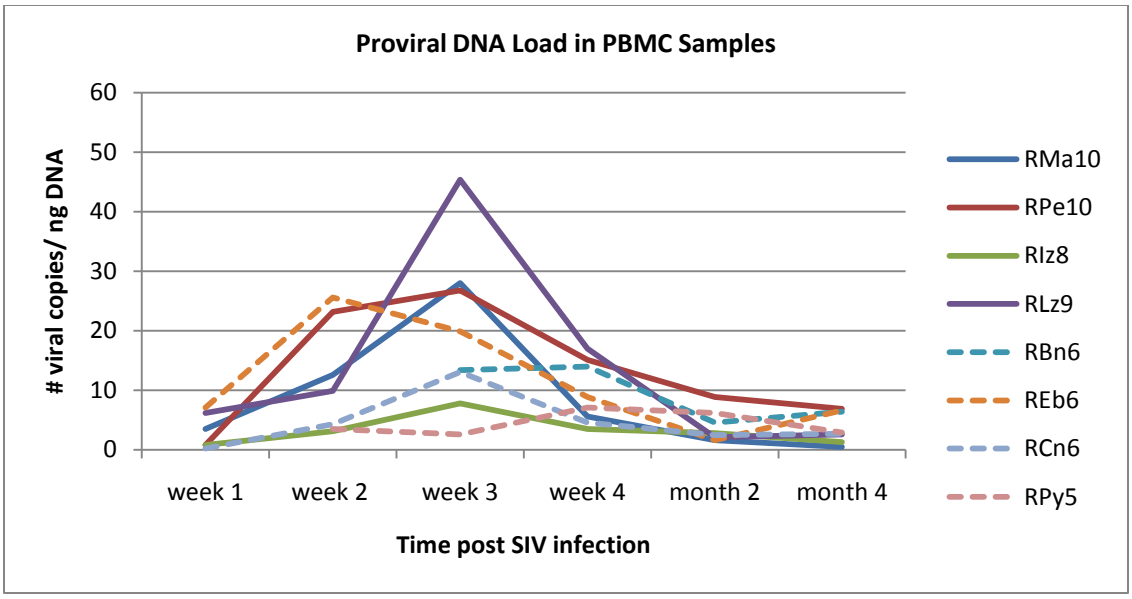

b)

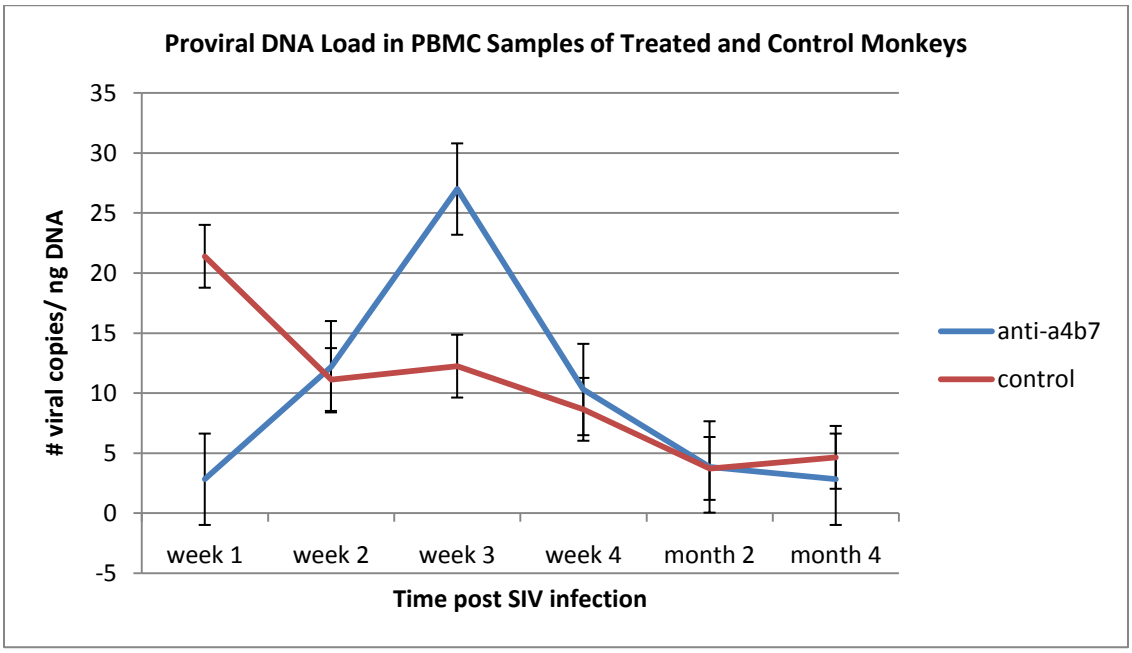

The proviral DNA levels in the isolated mononuclear cells from the gut tissue showed a much clearer difference in the levels between the anti-$\alpha 4\beta 7$ monkeys and the control monkeys (Fig 2a). The mean levels of proviral DNA in the mononuclear cells isolated from the jejunal tissue from the anti-$\alpha 4\beta 7$ treated monkeys were lower (peak mean level, 1.435 copies/ng DNA)

than the proviral DNA levels in the control monkeys (peak mean level,6.375 copies/ng DNA) (Fig 2b). In both the treated and control monkeys, the proviral DNA load in the jejunal mononuclear cells increased at week 2, and then steadily decreased at month 2 and 4. In the treated monkeys however, this decrease lead to an almost undetectable level of proviral DNA, but the control monkeys maintained a low, but detectable, level of proviral DNA (mean value at month 4, 0.86 copies/ng DNA).

Figure 2.

Levels of proviral DNA expressed as copies per nanogram of DNA extracted from mononuclear cells from each of the four anti-α4β7 mAb-treated animals and the four control animals from jejunal biopsies. Proviral loads are shown individually by monkey (a) and by each experimental group (b) with the anti-a4b7 treated monkeys being the solid lines and the control groups as the broken lines. Standard error bars are shown for each group of monkeys. The peak levels of proviral DNA loads in the jejunal and colorectal tissues in the α4β7-treated animals are statistically different (p = 0.021) from the same tissues of the control animals.

a)

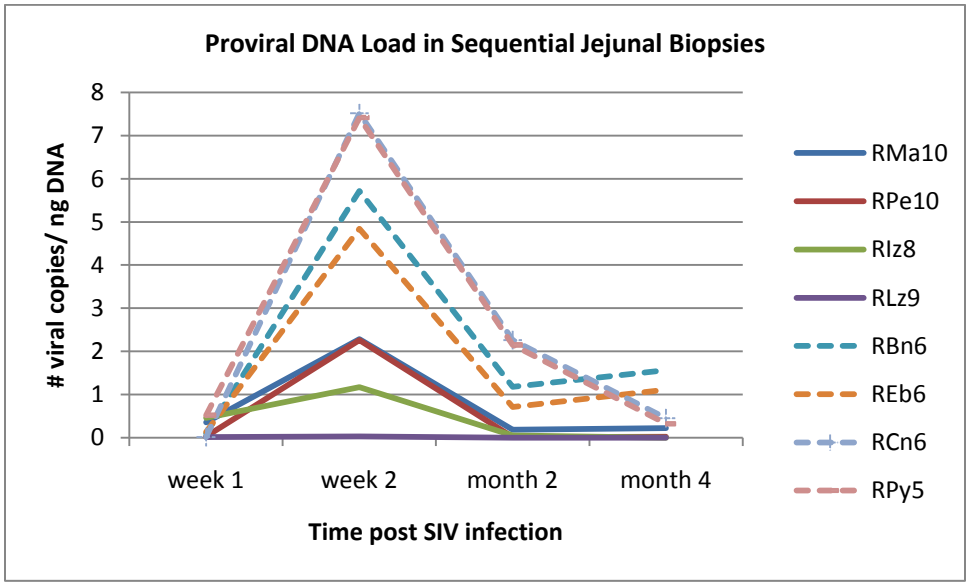

b)

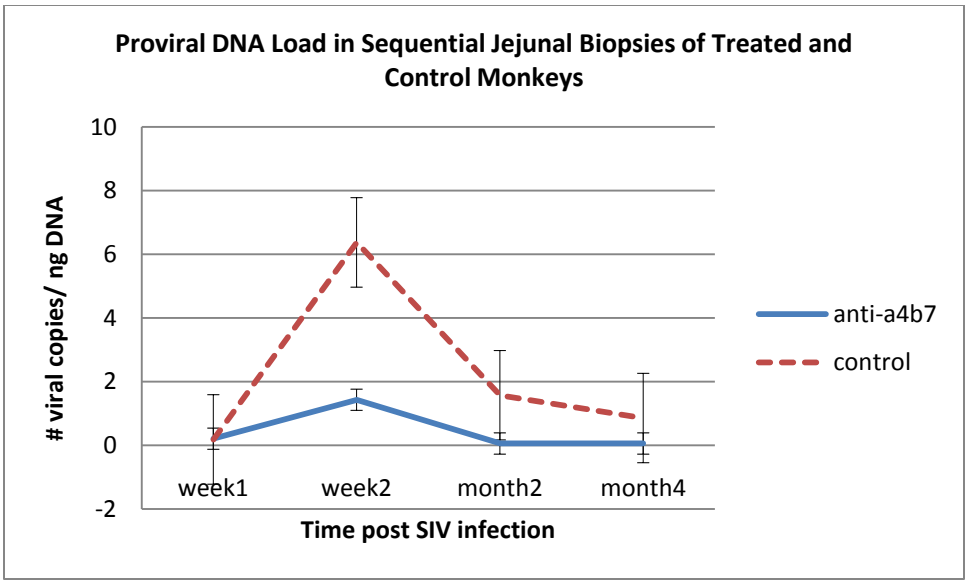

The proviral DNA levels in the colorectal tissues followed a similar pattern of viral loads as noted for the jejunal samples between the control and anti-α4β7 treated monkeys. The levels of proviral DNA in the mononuclear cells of the colorectal tissue in the anti-α4β7 treated monkeys were lower (peak mean level, .7275 copies/ ng DNA) than the proviral DNA loads in the control monkeys (peak mean level, 12.61 copies/ng DNA) (Fig 3a). In the control monkeys, the proviral DNA loads in the mononuclear cells of the colorectal tissue were high at week one post infection, and then gradually decreased until the proviral load reached a steady level at month 4 (mean value, 1.354 copies/ng DNA). The mononuclear cells of the colorectal tissue of the treated monkeys, on the other hand, maintained a low and almost undetectable level of proviral DNA, reaching a minor peak at week 2 (mean value, 0.7275 copies/ng DNA) (Fig 3b).

Figure 3.

Levels of proviral DNA expressed as copies per nanogram of DNA extracted from mononuclear cells from each of the four anti-α4β7 mAb-treated animals and the four control animals from colorectal biopsies. Proviral loads are shown individually by monkey (a) and by each experimental group (b) with the anti-a4b7 treated monkeys being the solid lines and the control groups as the broken lines. Standard error bars are shown

for each group of monkeys. The peak levels of proviral DNA loads in the jejunal and colorectal tissues in the α4β7-treated animals are statistically different ($p = 0.021$) from the same tissues of the control animals.

a)

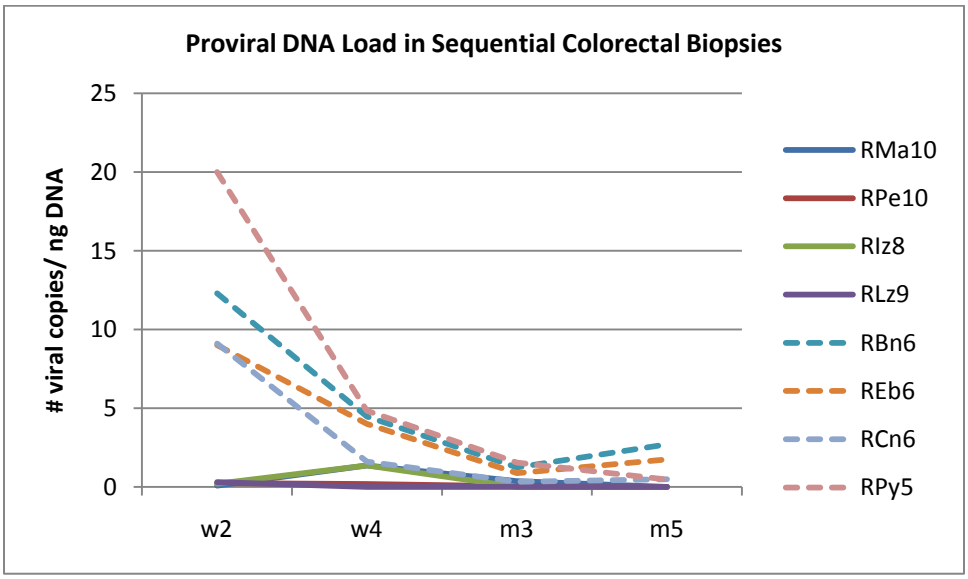

b)

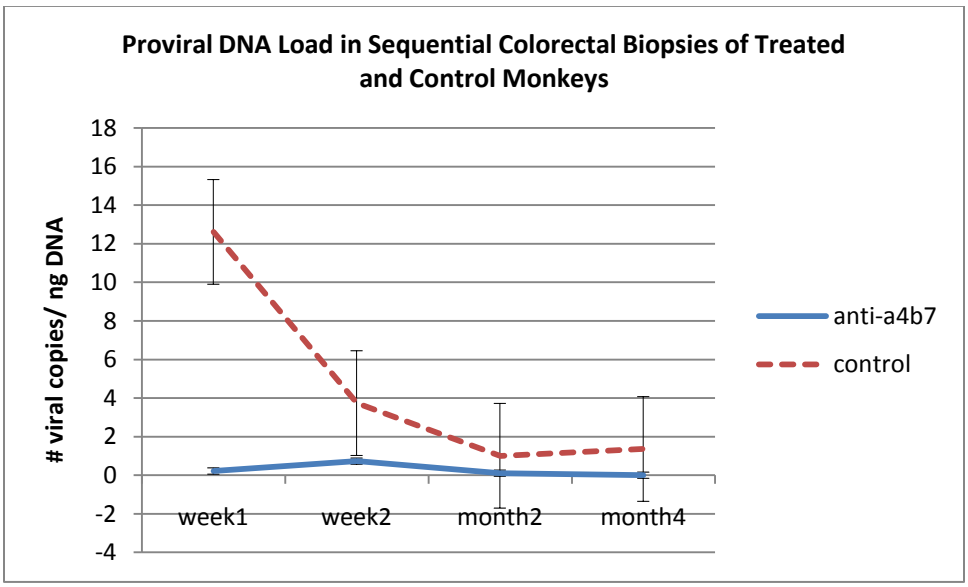

Overall, there was a lower level of proviral DNA in the jejunal tissues than in the colorectal tissues. This may be mainly due to the fact that the colorectal tissues comprise of a much higher number of lymphoid cell aggregates than the jejunum. Because of this difference, a

much higher yield of mononuclear cells is obtained in the colorectal biopsies than in an equivalent amount of jejunal tissue biopsy.

It is important to note that in both the mononuclear cells of the jejunal and colorectal tissues, the proviral DNA levels in the control monkeys maintained a higher level of proviral DNA over the course of infection. These data suggest the anti-$\alpha4\beta7$ mAb administration reduces the level of viremia and the frequency of provirus-infected CD4+ T cells within the GI tissues during acute infection.

The Kinetics of Various Transcription Factor and Cytokine mRNA in jejunal biopsies during acute SIVmac239 infection in anti-alpha4/beta7 treated and control monkeys.

The relative levels of mRNA coding for a number of select transcription factors and cytokines from mononuclear cells from jejunal and colorectal biopsies were analyzed from both the anti-$\alpha4\beta7$ mAb-treated monkeys and the control monkeys.

In the jejunal biopsies of the anti-$\alpha4\beta7$ mAb treated monkeys, the levels of mRNA coding for FOXP3 (Fig. 4a), IL-17A (Fig. 4c), ROR-Cγ (Fig. 4d), IL-21 (Fig. 4e), IL-22 (Fig. 4f), and MIP-3α (Fig. 4h) showed little or no change during the acute infection period (up to week 10 post infection). The mRNA coding for IL-23 (Fig. 4g) experienced a slight increase during this acute infection period and GARP (Fig. 4b) experienced a decrease in level during this period. The levels for IL-17A, ROR-Cγ, IL-21, IL-22, and IL-23 at 4 months post infection all experienced a sharp decline while GARP and FOXP3 remained at the same level and the levels of MIP3α increased during this period.

In the jejunal biopsies of the control group on the other hand, the mRNA coding for FOXP3, GARP, IL-21, IL-23, and MIP-3α all showed a sharp initial increase, and the mRNA coding

for IL-17A, ROR-Cγ, and IL-23 all showed a sharp initial decrease during the acute infection period. At 4 months post infection, all the mRNA levels stayed at low levels except for levels of IL-23, which showed an increase (Fig. 4).

Figure 4.

The relative levels of mRNA specific for FOXP3, GARP, IL-17A, ROR-Cγ, IL-21, IL-22, IL-23 and MIP-3α in samples isolated from jejunal biopsies isolated from four animals treated with the anti-α4β7 mAB (solid lines) and four control monkeys (broken lines). Data is shown as median values with standard error bars for each data set. The value obtained from baseline is denoted as 1. The DDCT values are based on β_2-microglobulin levels or GAPDH levels and levels of mRNA from baseline values from the same monkey.

a)

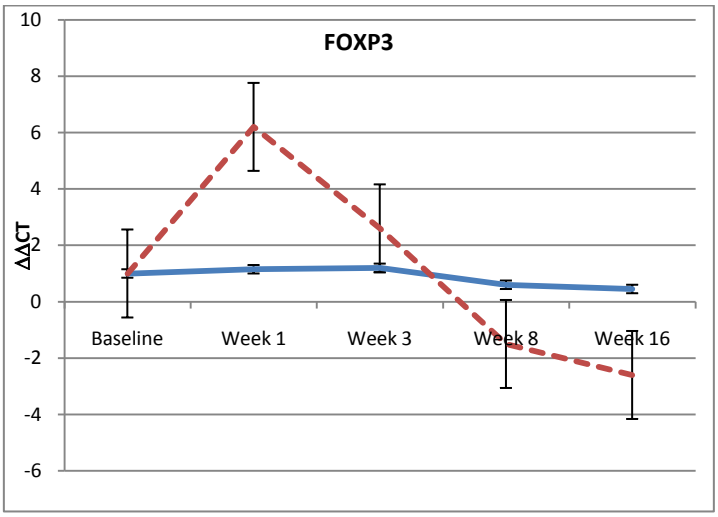

b)

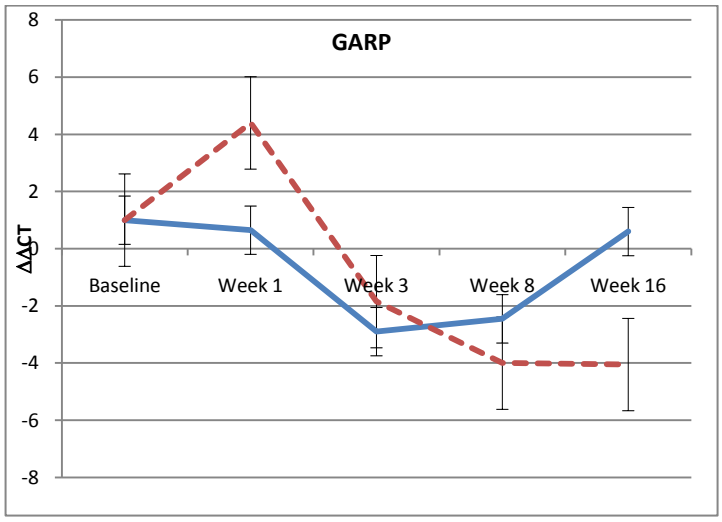

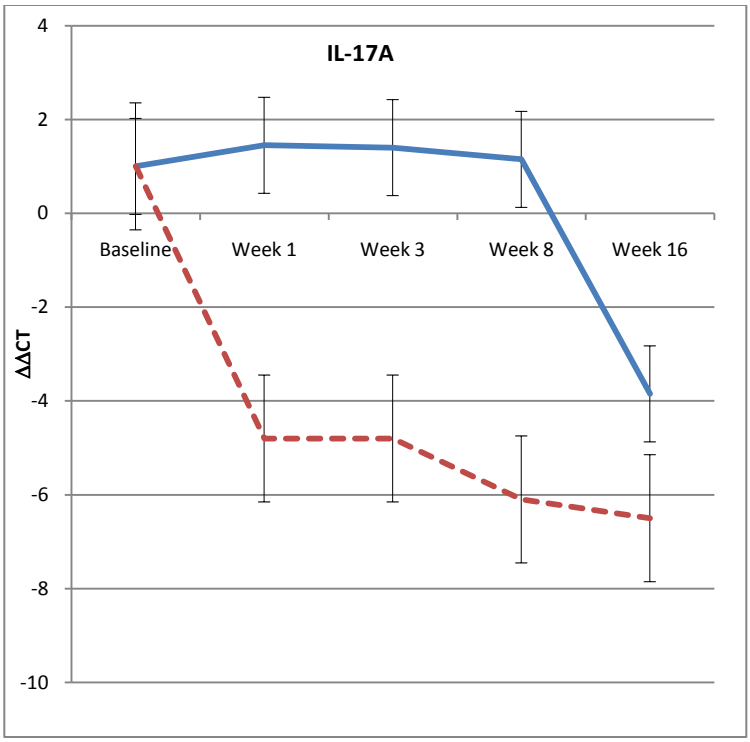
IL-17A
4
2
0
-2
-4
-6
-8
-10
ΔΔCT
Baseline
Week 1
Week 3
Week 8
Week 16

c)

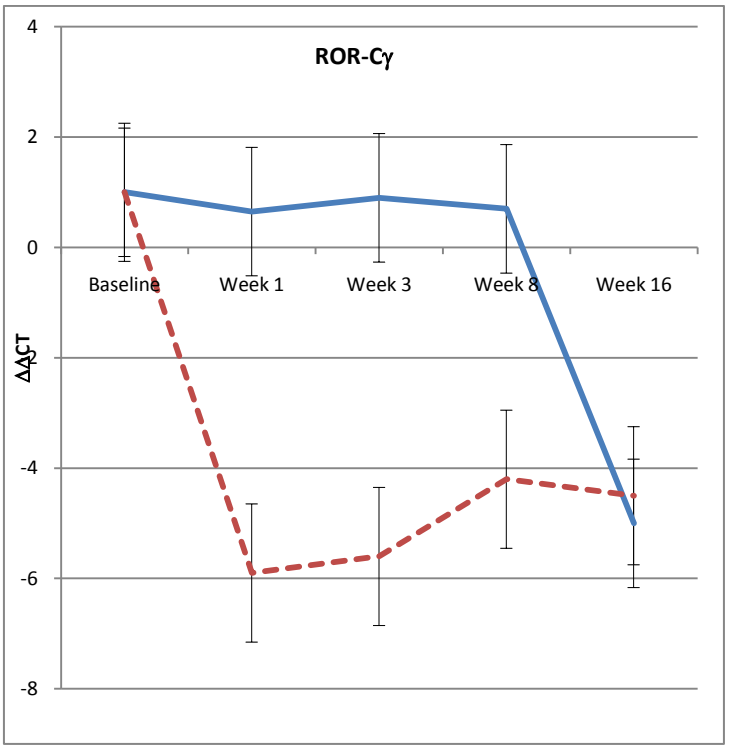
ROR-Cγ
4
2
0
-2
-4
-6
-8
ΔΔCT
Baseline
Week 1
Week 3
Week 8
Week 16

d)

Figure 4 (continued).

e)

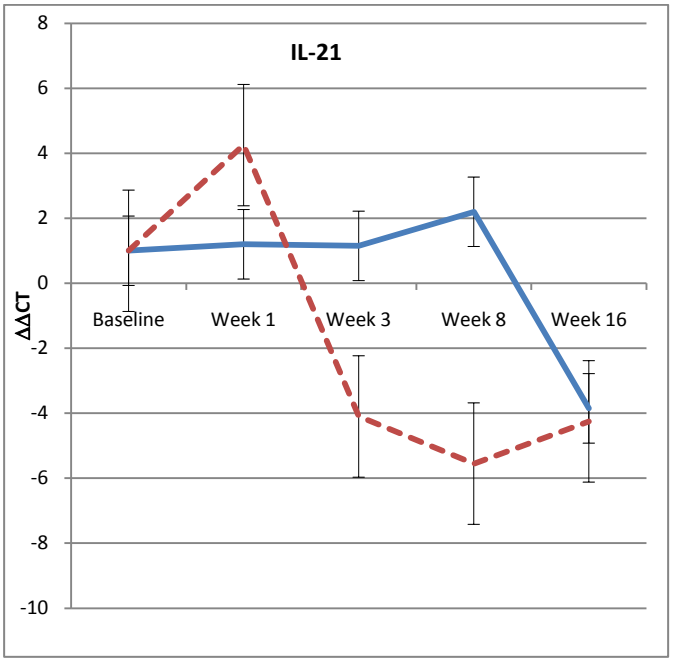

f)

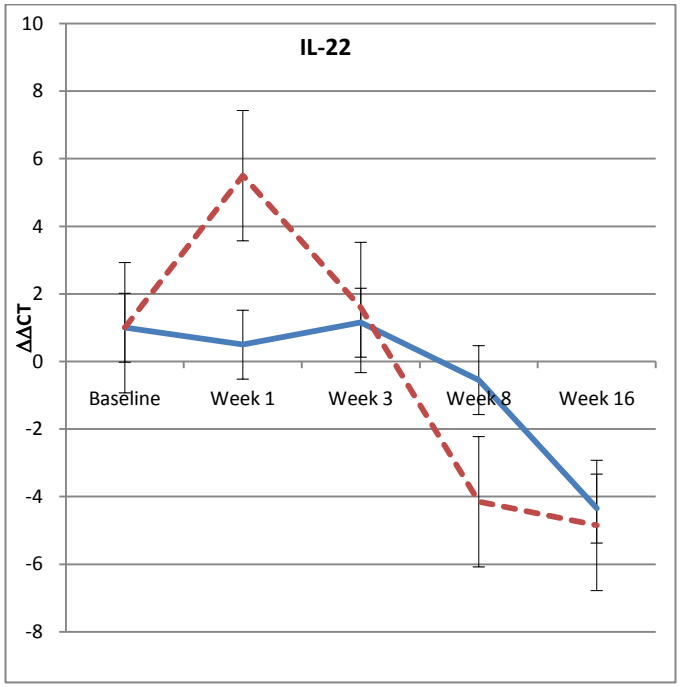

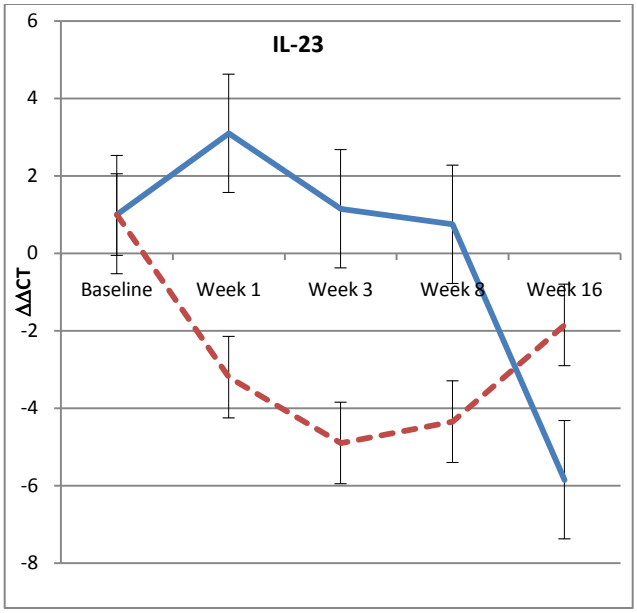

g)

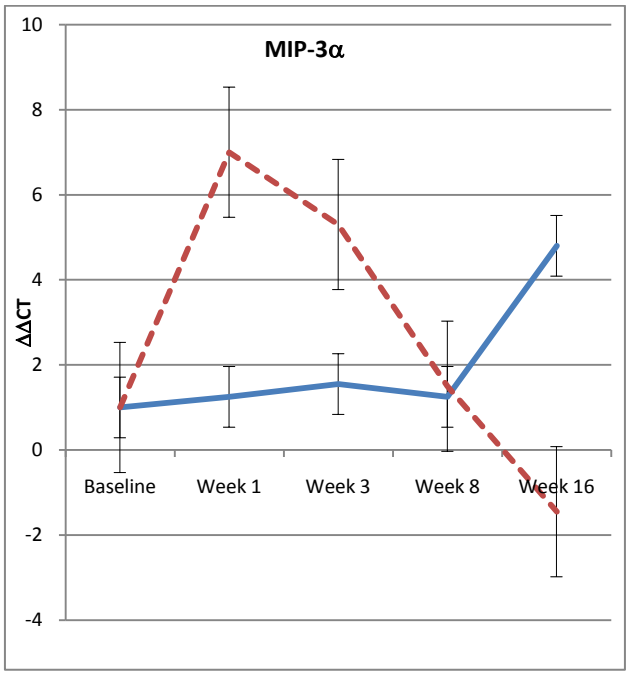

h)

In the colorectal biopsies, the patterns of changes of mRNA values for GARP (Fig. 5b) and MIP-3α (Fig. 5h) were similar to the jejunal biopsies for both the treated and control groups.

In the control monkeys, the pattern of mRNA values between jejunal and colorectal biopsies were similar for all the transcription factors and cytokines except for IL-23, where the colorectal samples experienced a sharp initial increase and then a dramatic decline (Fig. 5g). In the treated monkeys, the pattern of mRNA values were similar between colorectal and jejunal biopsies for IL-23 and ROR-Cγ (Fig. 5d). The colorectal tissue of the treated monkeys experienced an increase in levels of IL-21 (Fig. 5e) and IL-22 (Fig. 5f) compared to their jejunal counterparts, while FOXP3 (Fig. 5a) levels were significantly lower during acute infection and then experienced a significant increase at the 4 month level. The levels of IL-17A (Fig. 5c) in the colorectal tissue of the treated monkeys are similar to the jejunal tissue during acute infection, but do not experience the sharp decline in levels as they do in the jejunal tissue.

The difference between colorectal and jejunal mRNA levels may be due to the fact that the number of lymphoid cell aggregates in colorectal tissue are higher.

Figure 5.

The relative levels of mRNA specific for FOXP3, GARP, IL-17A, ROR-Cγ, IL-21, IL-22, IL-23 and MIP-3α in samples isolated from colorectal biopsies isolated from four animals treated with the anti-α4β7 mAB (solid lines) and four control monkeys (broken lines). Data is shown as median values with standard error bars for each data set. The value obtained from baseline is denoted as 1. The DDCT values are based on β_2-microglobulin levels or GAPDH levels and levels of mRNA from baseline values from the same monkey.

a)

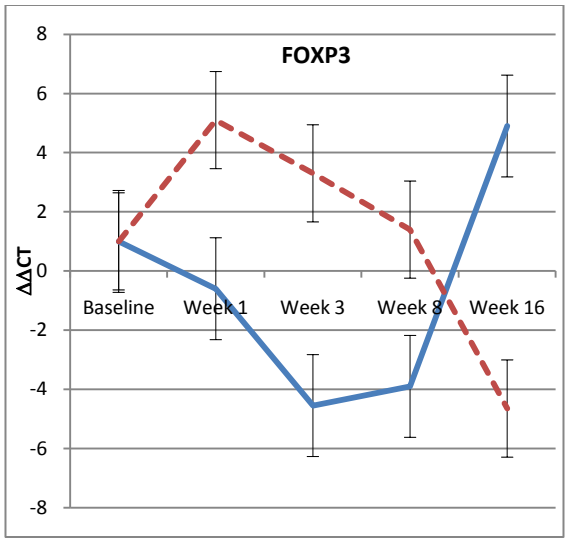
FOXP3
8
6
4
2
0
-2
-4
-6
-8
ΔΔCT
Baseline
Week 1
Week 3
Week 8
Week 16

b)

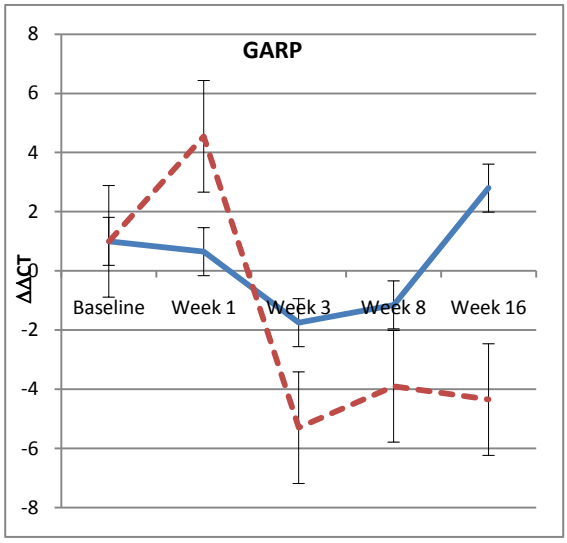
GARP
8
6
4
2
0
-2
-4
-6
-8
ΔΔCT
Baseline
Week 1
Week 3
Week 8
Week 16

c)

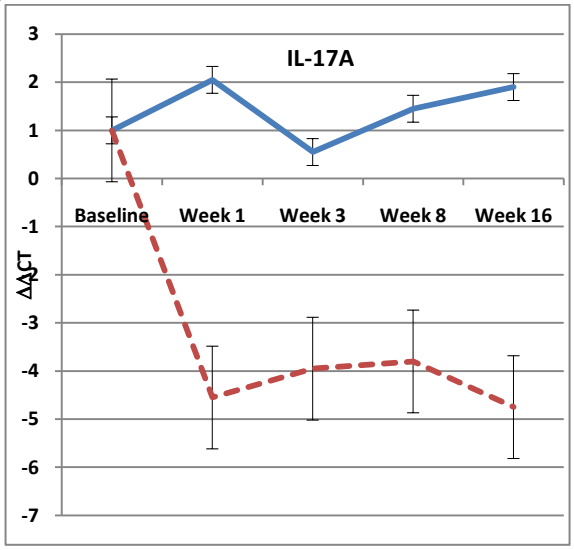
IL-17A
3
2
1
0
-1
-2
-3
-4
-5
-6
-7
ΔΔCT
Baseline
Week 1
Week 3
Week 8
Week 16

d)

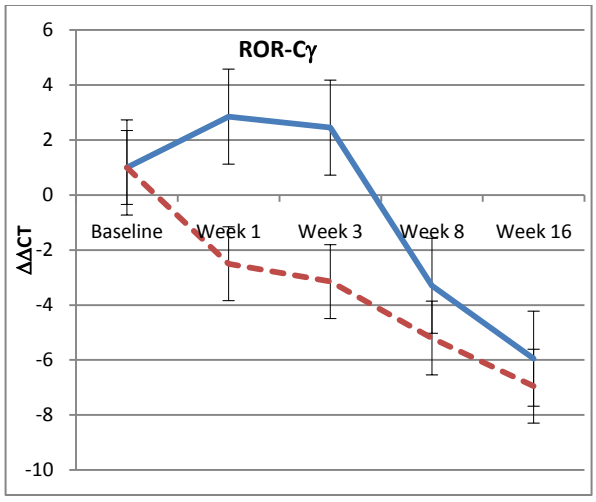
ROR-Cγ
ΔΔCT
6
4
2
0
-2
-4
-6
-8
-10
Baseline
Week 1
Week 3
Week 8
Week 16

e)

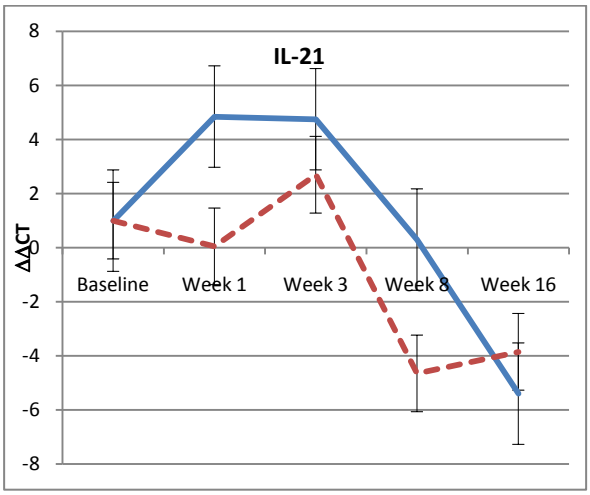
IL-21
ΔΔCT
8
6
4
2
0
-2
-4
-6
-8
Baseline
Week 1
Week 3
Week 8
Week 16

f)

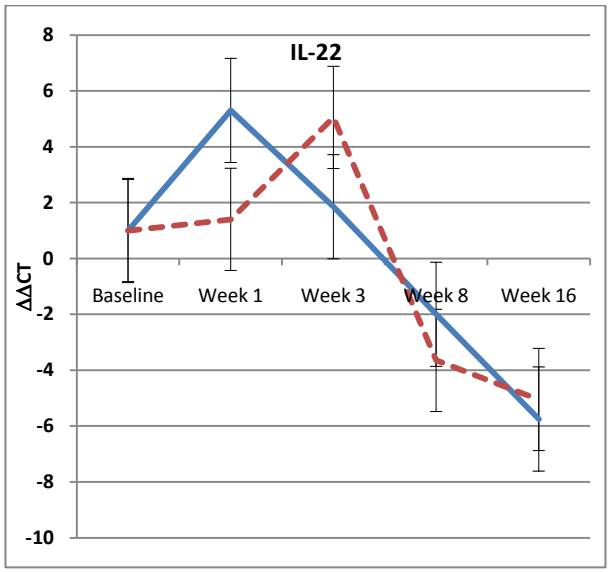
IL-22
ΔΔCT
8
6
4
2
0
-2
-4
-6
-8
-10
Baseline
Week 1
Week 3
Week 8
Week 16

g)

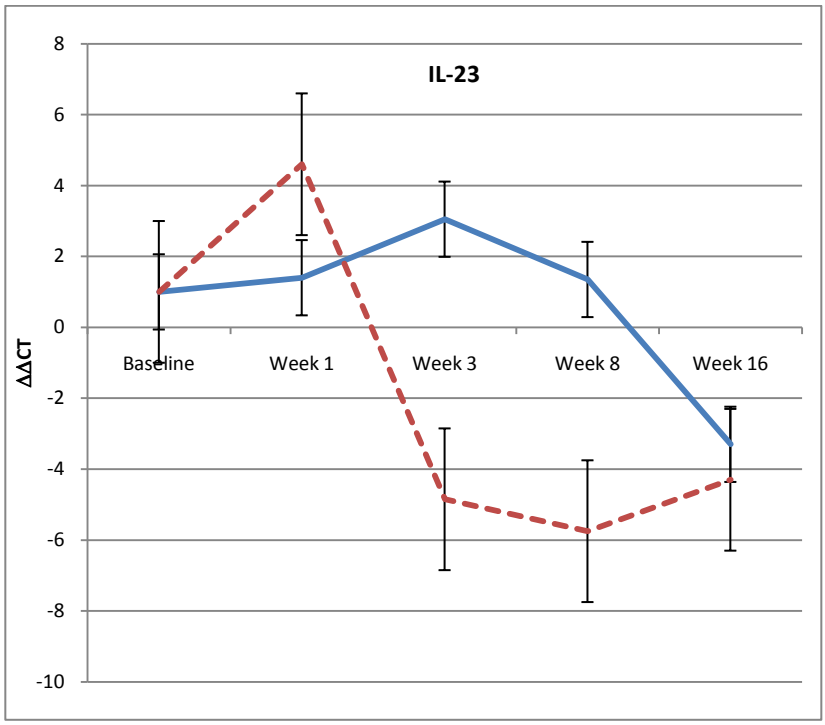
IL-23
8
6
4
2
0
-2
-4
-6
-8
-10
ΔΔCT
Baseline
Week 1
Week 3
Week 8
Week 16

h)

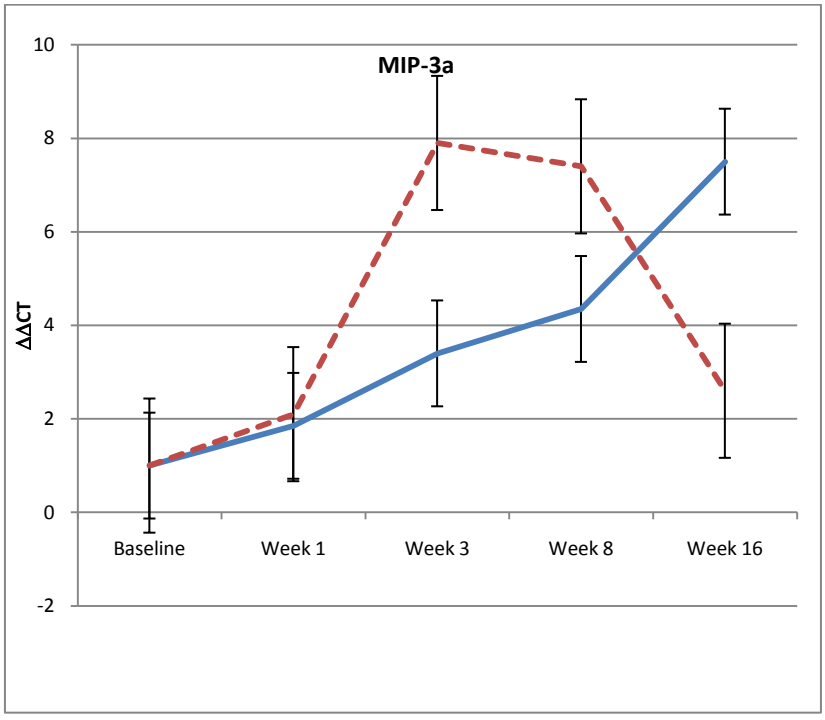
MIP-3a
10
8
6
4
2
0
-2
ΔΔCT
Baseline
Week 1
Week 3
Week 8
Week 16

Effect of in vivo anti-α4β7 mAb infusion on plasma levels of IL-10, IL-7, IL-15, TGF-β, and IFN-α:

The concentrations of the cytokines IL-10, IL-7, IL-15, TGF-β and IFN-α were quantified using plasma samples from both the anti-a4b7 treated monkeys and the control monkeys.

The plasma levels of IL-10 were higher in samples from the control group overall, although both the control and the a4b7 treated groups did experience a peak at week 1 post infection (Fig. 6a). The treated group maintained a relatively constant level after this peak while the control group experienced a significant drop and then a slight increase by 4 months post infection.

The plasma levels of IL-7 were higher for the anti-α4β7 treated group overall, showing a slight drop at week 1 and then a steady rise thereafter (Fig. 6b). The control group showed decreasing levels overall, dropping towards undetectable levels by 4 months post infection.

The plasma levels of IL-15 were undetectable for each of the samples from all of the monkeys at all time points examined. It is possible that this cytokine is used up in an autocrine fashion making it difficult to quantify levels being synthesized.

The plasma levels of TGF-β showed a decreasing trend for both the treated and control groups in the acute infection period, although the control group drop in concentration was much more dramatic. Also, the treated group showed an increase in level by 4 months post infection (Fig. 6c).

The levels and trend in changes of concentration for IFN-α were very similar for both the treated and control group, showing a sharp peak at week 1 post infection (Fig. 6d).

Figure 6.

The concentration (pg/mL) of IL-10, IL-7, TGF-β, and IFN-α in plasma samples isolated from 4 monkeys treated with anti-a4b7 mAB (solid lines) and four control monkeys (broken lines). Data is shown as mean values with standard error bars for each data set.

a)

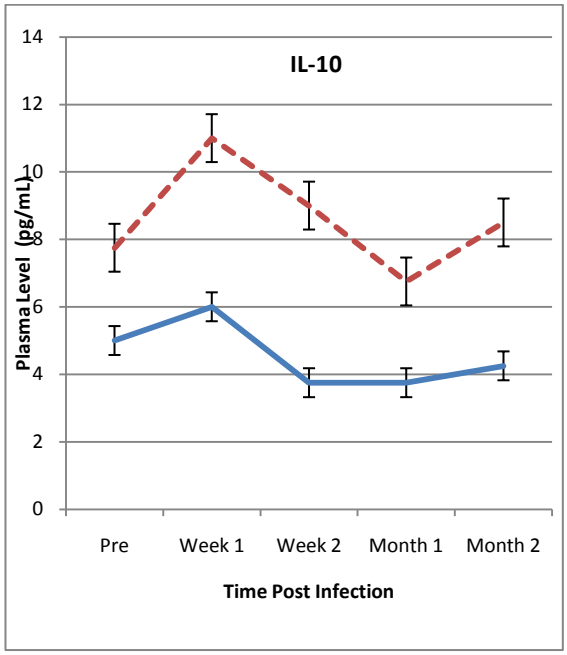

b)

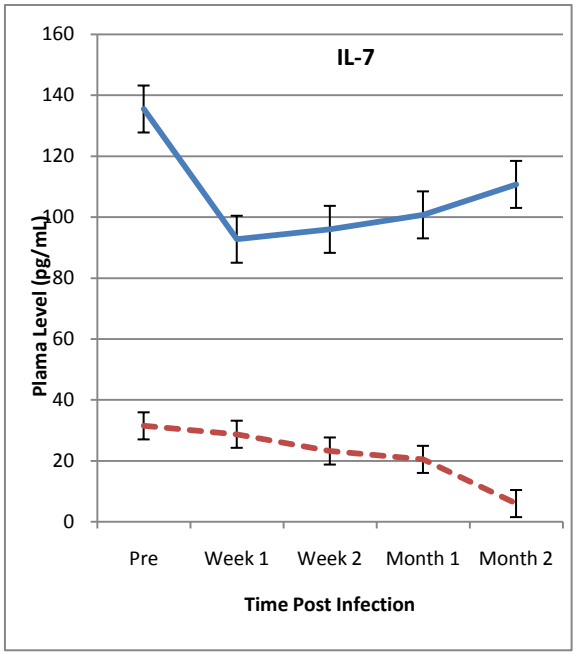

c)

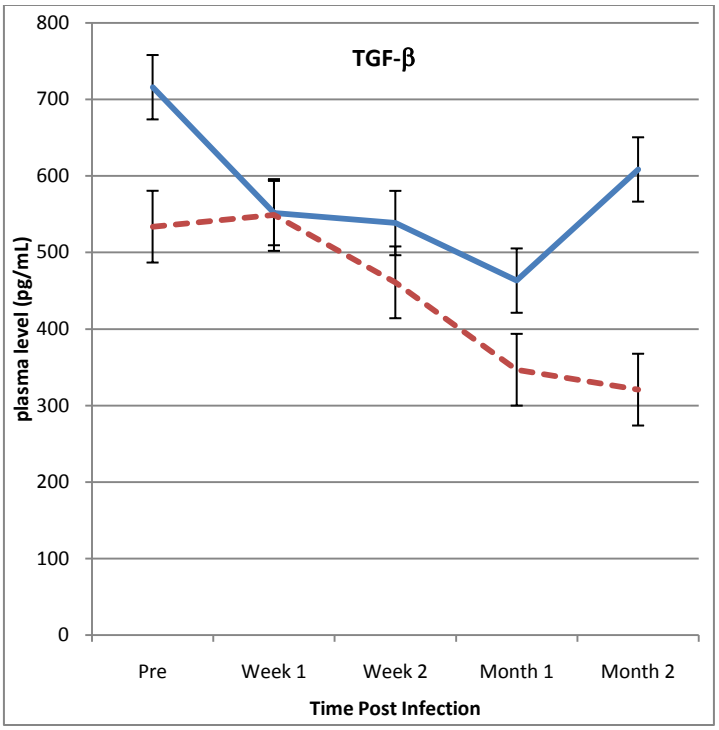
TGF-β
plasma level (pg/mL)
800
700
600
500
400
300
200
100
0
Pre
Week 1
Week 2
Month 1
Month 2
Time Post Infection

d)

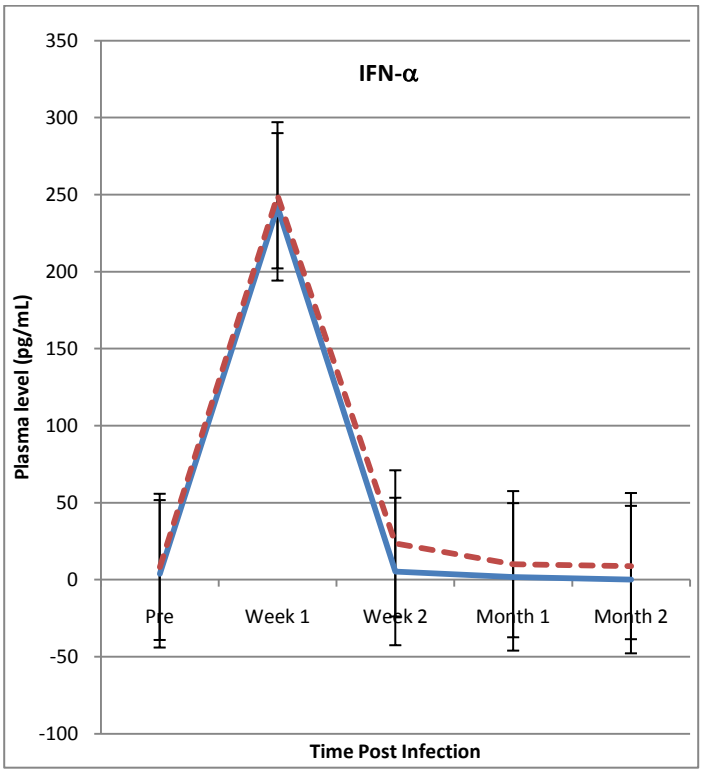
IFN-α
Plasma level (pg/mL)
350
300
250
200
150
100
50
0
-50
-100
Pre
Week 1
Week 2
Month 1
Month 2
Time Post Infection

Discussion

The administration of anti-$\alpha4\beta7$ mAb to SIV infected rhesus macaques was used by our lab as a potential tool to either block SIV infection and/or prevent the trafficking of $\alpha4\beta7$ expressing cells in attempts to better understand the role of the $\alpha4\beta7$ integrin in acute SIV infection. To fully analyze the effects of the $\alpha4\beta7$ integrin on viral loads, we collected data measuring the levels of plasma viremia, proviral DNA load in PBMCs and the mononuclear cells of the jejunum and colorectum. In addition to the proviral data, we collected data measuring the relative expression of mRNA levels of a select number of cytokines and transcription factors in the gut as well as the level of plasma cytokines from the $\alpha4\beta7$ treated and control animals in efforts to establish immunological correlates of the $\alpha4\beta7$ treatment.

To fully understand my data, it is imperative to bring the results of my study in light of the larger data set collected by our lab with respect to the anti-$\alpha4\beta7$ mAb treatment. As expected in light of the proviral DNA data presented above, the plasma viral load data collected (Supplemental Figure 1a) shows both a lower peak plasma viremia level and a lower viral set point at week 10 post infection for the anti-a4b7 mAb treated monkeys compared to the control monkeys (treated monkeys: peak= 4 x 10^6 copies/mL of plasma, set point= <100,000 copies/mL of plasma; control monkeys: peak= >32 x 10^6 copies/mL of plasma, set point= >1,000,000 copies/mL of plasma). The differences in plasma viral load between the two groups is even more marked when the viral load is analyzed as a reflection of the number of CD4(+) T cells (Supplemental Figure 1b). Also, the colorectal and jejunal levels of viral RNA (Supplemental Figures 1c and 1d) are markedly lower in the anti-$\alpha4\beta7$ mAb treated group than in the control group. Just as with the proviral DNA loads in the mononuclear cells of the colorectal and jejunal tissue, the viral load in the colorectal cells are higher than in the jejunal cells, probably because of the higher number of lymphoid aggregates present in the colorectal tissue. Another

significant phenomenon observed in the study is that there is a higher absolute number of CD4(+)T cells in the treated monkeys compared to the control monkeys (Supplemental Figure 2). This shows that the anti-a4b7 treatment prevents the depletion of circulating blood CD4(+) T cells. Also important to mention are the frequencies and absolute number of peripheral blood CCR5(+) CD4(+) T cells, the major target of SIV infection, in the anti-$\alpha 4\beta 7$ mAb treated monkeys. Although all the monkeys demonstrated a drop in CCR5(+) CD4(+) T cells, the treated monkeys showed a recovery of these cells by week 6 post infection (Supplemental Figure 3). A last important observation made by our lab was that the frequency of CD4(+) T cells in jejunal and colorectal tissue was higher in the anti-a4b7 mAb treated monkeys than in the control monkeys (Top panel of Supplemental Figure 4). These data once again suggest the protective quality of the anti-$\alpha 4\beta 7$ mAb treatment against SIV infection of resident CD4(+) T cells in the gut.

What remains unclear is whether the anti-a4b7 mAb reached all of the target tissue and cells effectively. The GALT hosts 70% of all the lymphoid cells in the body so complete blocking of the $\alpha 4\beta 7$ integrin on all these cells seems ambitious[xx]; however our lab found nearly complete blocking on cells isolated from jejunal and colorectal tissues of the treated monkeys. The protective quality established by the lower proviral DNA and plasma viral loads and the retention of the CD4(+) T cells in the treated monkeys is clear, however the mechanism behind this protective quality of anti-$\alpha 4\beta 7$ mAb treatment is still unclear. The potential explanations behind this protective phenomenon are that the mAb could be either blocking the trafficking of the $\alpha 4\beta 7$ expressing cells in the animals, inhibiting the function of these cells by blocking signaling mechanisms, or it could actually be blocking the virus's ability to enter and infect cells. From data collected from our lab, it is shown that this mAb is not lytic and therefore the depletion hypothesis is not valid. Evidence exists supporting both the trafficking hypothesis and the blocking hypothesis. For example, the anti-$\alpha 4\beta 7$ mAb is shown to inhibit the adhesion of the

$\alpha 4\beta 7$ integrin to its cognate MAdCAM-1 ligand.[xxi] This inhibition would interfere with the homing mechanism of cells expressing the $\alpha 4\beta 7$ integrin to travel to the gut. On the other hand, it has been shown that the anti-$\alpha 4\beta 7$ Ab inhibits the binding of HIV gp120 to the $\alpha 4\beta 7$ integrin.[xxii] This suggests that the Ab treatment is preventing SIV viral infection of the cells. Although both hypotheses are valid, further analysis is required to determine the exact mechanism that is occurring to provide protection against high viral loads seen in the control monkeys.

Another interesting question raised from the data collected concerns the level of virus present in the treated monkeys. Although the treated monkeys did have lower plasma viral loads and proviral DNA loads than the control group, the monkeys still showed a significant presence of SIV virus in their systems. Also, the peak of viremia is concurrent with CD4(+)T cell depletion in the gut. This combined with the fact that there is a recovery of CCR5(+) CD4(+) T cells in the treated monkeys suggests that the anti-$\alpha 4\beta 7$ treatment has some degree of protective quality on these traditionally highly susceptible cells in appropriate target tissues. This decrease in susceptibility of infection for CD4(+) T cells in the gut suggests that the virus is replicating elsewhere in the body and the mechanisms and locations in the body associated with this replication are topics for further investigation.

To fully understand the immunological environment of the gut and correlates of $\alpha 4\beta 7$ induced biological effects, a deeper analysis of the synthesis and levels of key relevant transcription factors and cytokines is required. This analysis addresses the behavior of immune cell types that are not readily measureable with standard cell counting techniques, therefore the expression of transcription factors associated with the regulation of the cells are analyzed.

Regulatory T cells (Tregs) are important in their maintenance of immunological self tolerance through which the immune system can recognize self versus foreign antigens in the body and respond to each in an appropriate manner. These CD4(+) T cells work by suppressing the potentially harmful effects of effector T cells. [xxiii] Defects in Tregs have demonstrated severe autoimmune pathology, thus their maintenance in an organism is critical in regulating T cell homeostasis.[xxiv] Although their maintenance is important in preventing autoimmune diseases by maintaining self-tolerance, it has also been shown that an over activation of Tregs is phenotypically characteristic of certain immune deficient conditions.[xxv] In HIV/SIV infection in particular, Tregs are extremely important because of their ability to effectively suppress T cell activation and effector functions.[xxvi] In patients with HIV infection who demonstrate undetectable levels of viremia (HIV controllers), it has been shown that a low Treg response actually contributes to control of viral replication by promoting an effective adaptive immune response. [xxvii] To survey the activity of Tregs in our experimental model, we measured the levels of the transcription factors FOXP3 and GARP. FOXP3 is a master control gene for Tregs and is the most reliable marker for detecting Tregs. [xxviii] GARP mRNA is also expressed by activated Tregs and its expression correlates with the suppressive capacity of these cells.[xxix] In our experimental model, the monkeys who received anti-$\alpha 4\beta 7$ mAb treatment showed low levels of FOXP3 and GARP during the entire acute infection period in both the jejunal and colorectal samples as compared to the control monkeys who showed a sharp increase in FOXP3 and GARP expression at week 1 post infection. This suppression of FOXP3 and GARP is representative of the lack of a Treg response in the gut during early infection which may contribute to the low viremia and proviral levels seen in the treated animals. The suppression of a Treg response in the treated monkeys may allow for effector T cells to become activated and induce their

effector function against the SIV virus present in the gut, thus dampening the overall pathology associated with SIV infection.

A subset of CD4+ T cells that express IL-17 and termed Th17 cells are also important effector CD4(+) T cells that play a crucial role in regulating and initiating specific immune responses. Their important role in autoimmune disease and host protection against extracellular bacteria demonstrate why investigating their influence in the context of HIV/SIV infection is important.[xxx] Although Th17 cells have been shown to serve a pro-inflammatory function to help defend against foreign pathogens, their secretion of IL-17 also serves as an important factor in protecting the mucosal barrier function in the gut since this cytokine preserves the ultrastructure of the epithelial cells lining the gut wall.[xxxi] Th17 cells have also been shown to enhance the expression of antimicrobial peptides, an important line of defense against infection.[xxxii] In HIV infected individuals, it has been shown that there is preferential loss of Th17 cells and a loss in the balance between Th17 cells and Tregs.[xxxiii] This loss in Th17 cells correlates with chronic immune activation and severe HIV pathogenesis.[xxxiv] It has also been shown that long term non-progressors, or individuals who are HIV+ but do not develop severe HIV related pathogenesis, display a greater number of Th17 cells, thereby preserving the immune response against bacterial infection.[xxxv] In SIV infection, natural hosts of the virus like the sooty mangabey which do not develop the severe pathogenesis or AIDS , also seem to preserve the Th17 cell repository, suggesting the important role of mucosal immunity in preventing severe disease.[xxxvi] In SIV infected rhesus macaques, the loss of Th17 cells has been shown to be a crucial factor in chronic immune activation and disruption of mucosal immunity.[xxxvii] To identify the behavior of Th17 cells in our experimental model, we measured the relative mRNA expression of IL17A, a gene which encodes the cytokine IL17 that specifies the differentiation of effector T cells to the Th17 lineage. [xxxviii] We also chose to measure the level of expression of ROR-Cγ, a master

regulator transcription factor that regulates Th17 development.[xxxix] In our experimental model, there is a stark difference in the level of expression of IL-17A and ROR-Cγ between the anti-α4β7 mAb treated and control monkeys. In both the jejunal and colorectal tissue of the treated monkeys, an increase or maintenance in the level of these Th17 regulating genes are seen, while the control monkeys experience a drop in expression. This represents a continuing Th17 response in the anti-α4β7 mAb treated monkeys, which might maintain mucosal immunity against the SIV virus, thus allowing for viral clearance from the gut. The control monkeys lack the maintenance of their Th17 cells, which creates a vulnerable situation in the gut allowing for more SIV virus to infect gut cells.

Several cytokines are important in regulating immune responses as well as controlling viral infections. IL-21 is a key cytokine in inducing the maturation and differentiation of T, B, and NK cells and is produced by Th2 cells and Th17 cells.[xl] In HIV infected individuals, IL-21 has also been shown to play a role in enhancing the NK response, and these cytokine-activated NK cells further have been shown to inhibit viral replication.[xli] It has also been shown that HIV infection induces IL-21 synthesizing CD4(+) T cells and contribute to viral control via CD8(+) T cell maintenance.[xlii] In HIV-1 infected patients that are controllers of the HIV virus, specific IL-21 producing CD8(+) T cells have been shown to serve a critical role in viremia control.[xliii] In our experimental model, the treated monkeys showed a slight peak in IL-21 expression at the end of the acute infection period in the jejunal tissue, but in the colorectal tissue, there was a large increase in IL-21 expression over most of the acute infection period. The control monkeys (although there was a slight peak at week one post infection in the jejunal tissue) showed a lower level of expression of IL-21 compared to the anti-α4β7 mAb treated monkeys. Although IL-21 is involved in the proliferation of NK cells, in our model it seems that this function of IL-21 was not occurring. According to data collected in our lab (Supplemental Figures 5a and 5b),

there was a significant increase in the absolute numbers of NK cells in the control animals that is absent in the treated animals. Instead, this increase in IL-21 in the anti-$\alpha 4\beta 7$ mAb treated animals may be due to the fact that there are more IL-21 producing CD4(+) T cells and Th17 cells in the treated group than in the control animals. In addition, the IL-21 produced by CD8(+) T cells which are involved in viremia control may also account for the increase in production. Data collected in our lab (Supplemental Figure 4) shows an increased in the number of CD8(+) T cells entering the jejunal and colorectal tissues.

Another important cytokine involved in infection is IL-22. IL-22 is involved in inflammatory regulation at mucosal surfaces, and thus its role in HIV/SIV infection is important to report.[xliv] Acting through innate immune systems, IL-22 has been shown to serve an important role in HIV host-resistance to infection.[xlv] It has also been shown that high systemic levels of IL-22 have been associated with low HIV replication in infected patients.[xlvi] In the jejunal tissue of our treated monkeys however, there was a consistently lower expression of IL-22 over the entire acute infection period compared to the control monkeys. In the colorectal tissue, both the control and the treated monkeys experienced a peak in expression, but the treated monkeys experienced this peak two weeks before the control monkeys did and then a significant drop in production. Although this pattern of low HIV viremia with high IL-22 expression does not follow data that has previously been reported in the literature, further analysis into the kinetics of IL-22 in anti-$\alpha 4\beta 7$ treated monkeys is needed. The suppression of production may also be representative of the fact that IL-22 is mainly produced by NK cells, and as previously mentioned, the anti-$\alpha 4\beta 7$ mAb treated monkeys showed a lower absolute number of NK cells compared to the control group.

A third important cytokine in the gut is IL-23. IL-23 induces a number of intestinal inflammatory pathways by restraining Treg responses and by inducing Th17 cytokine responses.[xlvii] It has also been shown that an excess of IL-23 promotes inflammatory bowel disease and intestinal tissue damage. [xlviii] In the context of HIV infection, it has been shown that there is a dominant IL-23 response during primary infection.[xlix] HIV is thought to subvert intestinal homeostatic mechanisms by activating innate immune receptors to induce IL-23, thereby inducing inflammation in the intestinal mucosa. [l] In the jejunal tissue of the anti-$\alpha4\beta7$ mAb treated monkeys, there is an increase in IL-23 production over the entire acute infection period; this is a stark contrast to the decrease in IL-23 production in the control monkeys. In the colorectal tissue, the control monkeys experience a slight peak at week 1 post infection in IL-23 expression, but then a dramatic decrease is seen over the rest of the course of infection. The anti-$\alpha4\beta7$ mAb treated monkeys however demonstrate an increase in IL-23 production in the later stages of acute infection. The overall increase of IL-23 production in the gut of the anti-$\alpha4\beta7$ mAb treated monkeys is reflective of other data collected in our lab concerning plamacytoid and myeloid dendritic cells (Supplemental Figure 6). Both of these cell lineages showed a decrease in absolute numbers, but the decrease was much more profound in the control group than in the anti-$\alpha4\beta7$ mAb treated group. Dendritic cells are major producers of IL-23[li], and this retention of dendritic cell number may represent the increase in IL-23 expression in the anti-$\alpha4\beta7$ mAb treated monkeys. However there is a major question as to the source of IL-23 production due to the next line of evidence concerning CCL20.

MIP-3α (or CCL20) is an important chemokine that stimulates the migration of dendritic cells (DC).[lii] In the context of HIV this DC tropic chemokine has been shown to persist at high levels throughout the course of HIV infection.[liii] In SIV infected macaques, it has been shown that there is a burst in the level of CCL20 during acute infection.[liv] In our experimental model, CCL20

synthesis is blocked in the jejunal tissue and there are marked lower levels in the colorectal tissue during acute infection. This is consistent with our hypothesis in that anti-$\alpha4\beta7$ mAb reduces the infiltration of DCs into the gut, thereby reducing the synthesis of CCL20. This however contradicts the pattern of IL-23 expression discussed earlier. In further evaluation, the levels of mDCs and pDCs in jejunal and colorectal biopsies were undetectable. This analysis supports the pattern of CCL20 suppression during acute infection in the anti-$\alpha4\beta7$ mAb treated monkeys, and demonstrates that the anti-$\alpha4\beta7$ treatment blocks DC infiltration into the gut. This leads to questions for further analysis about the source of the increase in IL-23 expression in the anti-$\alpha4\beta7$ mAb treated monkeys and why there is suppression of expression in the control monkeys.

IL-10 is an immunoregulatory cytokine that reduces the inflammatory response by suppressing cytokines and T cell proliferation. This immunosuppressive cytokine is produced and can affect a wide variety of immune cells, including B cells, NK cells, and dendritic cells.[lv] In many animal models, it has been shown that blocking this cytokine actually reduces viral persistence in chronically infected organisms.[lvi] In samples taken from HIV infected individuals, it has been shown that antibody blocking of the IL-10 pathway actually enhances CD4(+) responses.[lvii] It has also been shown that polymorphisms in the IL-10 gene leads to a form of IL-10 that reduces its expression, which correlates with a slower progression to clinical AIDS in HIV infected individuals.[lviii] The anti-$\alpha4\beta7$ mAb treated monkeys showed this same pattern of low IL-10 production compared to the control group. This lower production of IL-10 demonstrates that the immunosuppressive effects of the cytokine on effector immune cells are absent in the anti-$\alpha4\beta7$ mAb treated monkeys. These effector immune cells can therefore be more effective in clearing virus infecting cells of the host.

IL-7 is an important modulator in T cell survival and T cell homeostasis. IL-7 is also an essential part of T cell development and serves as a survival factor for T cells during development. It has been shown that mice that are IL-7(-) have a 20 fold decrease in thymic cells.[lix] Not only does IL-7 provide survival signals, but it helps maintain homeostatic levels of T cells, and when there is a situation of a depletion of T cells, it induces T cell expansion through co-stimulatory signals of the T cell receptor. IL-7 also delivers anti-apoptotic signals to thymic cells to ensure their survival.[lx] Because of its role in enhancing CD4(+) T cell numbers, IL-7 has been used as a therapeutic tool in SIV infected rhesus macaques to preserve naïve subsets of CD4(+) cells.[lxi] IL-7 has also been shown to reduce T cell apoptosis related to HIV infection.[lxii] In our experimental model, the anti-$\alpha 4\beta 7$ mAb treated animals had a significantly higher production of plasma IL-7 compared to the control group. This higher production is representative of the higher CD4(+) T cell counts and the increased number of CD8(+) T cells in the treated group.

TGF-β is an endogenous cytokine produced in the gut that is one of the most potent inhibitors of leukocyte activation. It is produced by every major leukocyte lineage and increased production of this cytokine is associated with immune defects and opportunistic infection.[lxiii] In the context of HIV infection, an increase in production of TGF-β is often associated with faster disease progression. This may be primarily because of its broad effects of inhibiting antiviral mechanisms, allowing an increase of viral infection of other cells. [lxiv] In our model, however, the anti-$\alpha 4\beta 7$ mAb treated monkeys, which showed lower viremia than the control group, produced a higher level of plasma TGF-β. This higher production may be representative of the muted inflammatory response that anti-$\alpha 4\beta 7$ treatment induces. By inhibiting the inflammatory response, the virus was unable to infect a large number of activated CD4(+) T cells, as it does in normal pathology.

IFN-α is a major cytokine in the body that signals a variety of antiviral mechanisms of the immune system. Early clinical trial of IFN-α as a therapeutic measure for patients who were HIV(+) gave seemingly positive results, due to IFN-α's antiviral and immunomodulatory effects.[lxv] But later studies proved that IFN-α poorly restricts HIV replication and the HIV's adaptive mechanisms for persistent infection proved stronger than IFN-α treatment.[lxvi] Studies in SIV infected Rhesus macaques have shown that IFN-α production did not inhibit viral replication.[lxvii] Although the effects of IFN-α in HIV infection are still being understood, it seems that in our experimental model, anti-α4β7 mAb treatment had no effect on IFN-α production. Both the control monkeys and the anti-α4β7 mAb treated monkeys showed a peak of IFN-α level in the plasma at week 1 post infection, which quickly diminished to undetectable levels by month 4.

Taken collectively, the data set regarding the anti-α4β7 mAb treatment in rhesus macaques leads to some definite conclusions, but also leads to many areas in need of further investigation. It is clear from the proviral DNA load data and the viral RNA load data collected that the anti-α4β7 mAb treatment reduces the level of viremia in the gut. When this data is considered in concert with the CD4+ T cell counts, which showed an increase in the frequency of CD4+ T cells in the anti-α4β7 mAb treated monkeys compared to the control monkeys, it suggests that the anti-α4β7 mAb treatment protects the CD4+ T cells from peripheral depletion. The fact that the traditionally highly targeted CCR5+ CD4+ T cells also show a recovery, in spite of significant viral loads, suggests that the anti-α4β7 mAb treatment decreases the susceptibility of these cells to SIV infection. However, the fact that there continues to be significant plasma viremia and pro-viral loads in the PBMCs indicate that there are significant levels of viremia in the anti-α4β7 treated animals. Thus, the high recovery of CD4+ T cells and the low gut viral and proviral loads elicit further investigation as to where in the body and in what cells of the body the SIV

virus is replicating in to maintain the viral loads seen in the treated monkeys. Also of importance to mention are the differences in NK cell and pDC frequencies in the anti-α4β7 mAb treated animals and the control animals. The anti–α4β7 mAb treatment mutes the NK and pDC response in the treated animals. Thus, while the control animals experience a large increase in the frequency of NK cells and pDCs circulating in the blood, this was not seen in the anti-α4β7 mAb treated animals. Other data collected in the lab demonstrated that there was also a pDC infiltration into the gut in the control animals that was not seen in the anti-α4β7 mAb treated animals. The anti-α4β7 mAb treatment seems to mute both of these inflammatory responses in the gut, which may be a key reason behind the dampened pathology and viremia in the anti-α4β7 mAb treated animals. This treatment opens the door to a powerful new method in understanding the kinetics of SIV/HIV infection. A more sustained administration of the anti-α4β7 mAb treatment is needed to fully understand the mechanism behind how the SIV virus causes gut pathology during acute infection.

There are still many key issues that remain to be defined concerning the translation of the anti-α4β7 mAb into a clinical setting. The primary issue worth investigating is whether anti-α4β7 mAb treatment sustains a significant clinical response in animals treated post-infection. In our experimental model, the animals were infected after the administration of the first dose of antibody, but a practical application of this treatment in a clinical setting would require the study of the effects of the antibody after SIV/HIV infection. A second clinically relevant model to study is the effect of the anti-α4β7 mAb on animals infected through a mucosal barrier (in our experimental model, the animals were infected intravenously), similar to how HIV is frequently transmitted in human populations. This would require the administration of the antibody to animals infected either intra-vaginally or intra-rectally, to mimic practical transmission modes of HIV in humans. A final model to study mimics human transmission: how would the antibody

administration effect viremia and pathology in animals that are repeatedly infected intra-vaginally with a low dose of SIV. The effectiveness of the anti-a4b7 mAb in all three of these situations is an important area for further research to develop a true sense of clinical relevance of this treatment.

Appendix

Figures and captions taken from: Ansari AA, Reimann KA, Mayne AE, Takahashi Y, Stephenson ST, Wang R, Wang X, Li J, Price AA, Little DM, Zaidi M, Lyles R, Villinger F. Blocking of α4β7 gut-homing integrin during acute infection leads to decreased plasma and gastrointestinal tissue viral loads in simian immunodeficiency virus-infected rhesus macaques. J Immunol. 2011 Jan 15;186(2):1044-59. Epub 2010 Dec 13.

Supplemental Figure 1

Effect of anti-α4β7 mAb treatment on plasma, jejunal, and colorectal tissue viral RNA loads of SIV-infected rhesus macaques. Data depict the viral RNA loads in samples from each of the four monkeys treated with the anti-α4β7 mAb (solid lines or bars) and each of the four control animals (broken lines or light bars) in blood and tissues. *A*, Kinetics of plasma VL in the anti-α4β7 mAb-treated and control monkeys. The median peak values in the α4β7-treated versus control animals are statistically different ($p = 0.021$). *B*, Plasma VL calculated relative to the corresponding absolute $CD4^+$ T cell counts in blood. *C*, Number of viral RNA copies in cells isolated from the jejunal tissues expressed as copies per nanogram of RNA and (*D*) number of viral RNA copies in cells from the colorectal tissues expressed as copies per nanogram of RNA. The median peak values for plasma VL, jejunal, and colorectal VL in the α4β7-treated versus plasma VL, jejunal, and colorectal VL in the control animals are each statistically different ($p = 0.021$).

a)

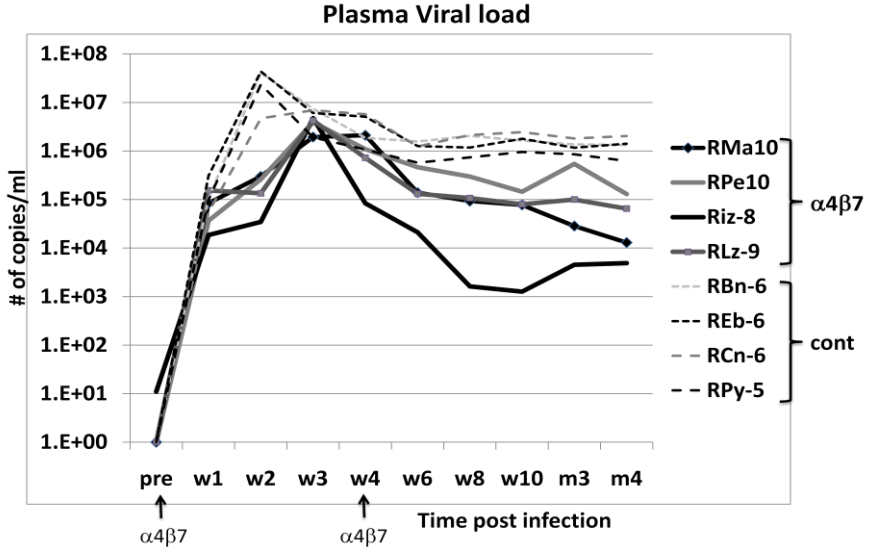

b)

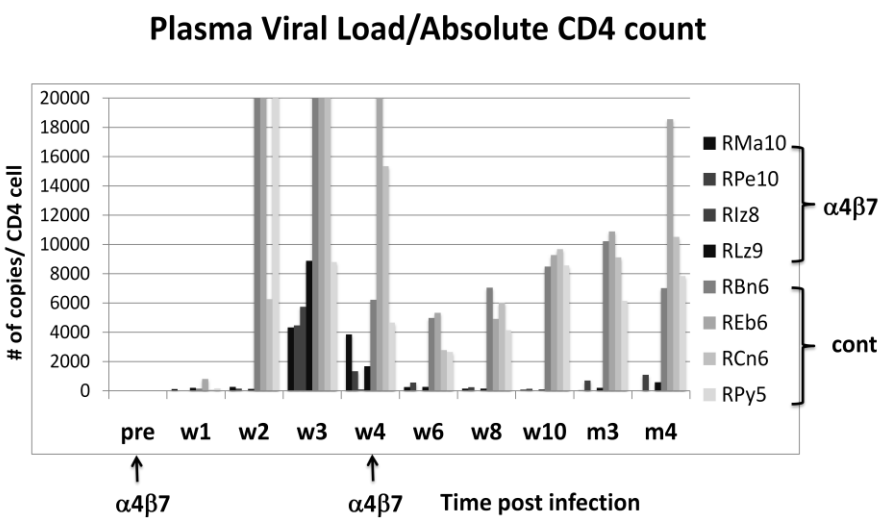
Plasma Viral Load/Absolute CD4 count
# of copies/ CD4 cell
20000
18000
16000
14000
12000
10000
8000
6000
4000
2000
0
RMa10
RPe10
RIz8
RLz9
RBn6
REb6
RCn6
RPy5
α4β7
cont
pre
w1
w2
w3
w4
w6
w8
w10
m3
m4
α4β7
α4β7
Time post infection

c)

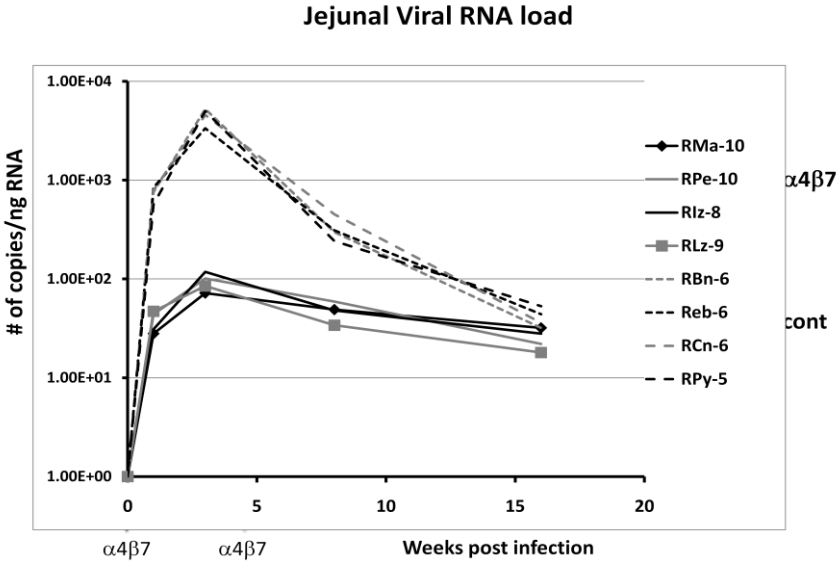
Jejunal Viral RNA load
# of copies/ng RNA
1.00E+04
1.00E+03
1.00E+02
1.00E+01
1.00E+00
0
5
10
15
20
RMa-10
RPe-10
RIz-8
RLz-9
RBn-6
Reb-6
RCn-6
RPy-5
α4β7
cont
α4β7
α4β7
Weeks post infection

d)

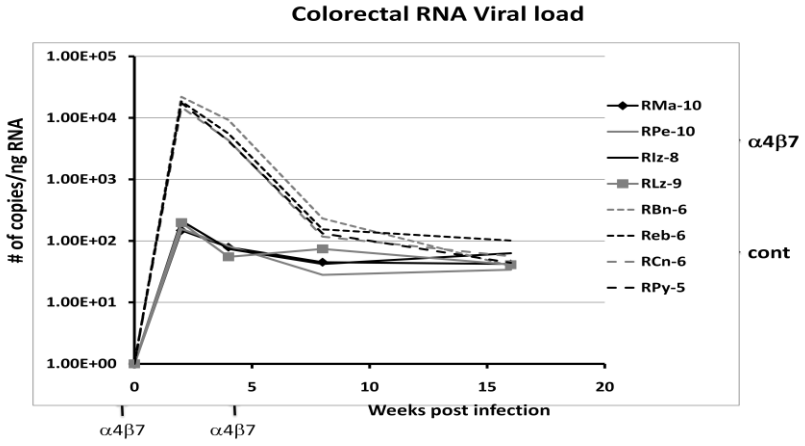
Colorectal RNA Viral load
# of copies/ng RNA
1.00E+05
1.00E+04
1.00E+03
1.00E+02
1.00E+01
1.00E+00
0
5
10
15
20
RMa-10
RPe-10
RIz-8
RLz-9
RBn-6
Reb-6
RCn-6
RPy-5
α4β7
cont
α4β7
α4β7
Weeks post infection

Supplemental Figure 2

Absolute numbers of peripheral blood $CD4^+$ T cells in samples from the four anti-α4β7 mAb-treated animals (solid lines) and the four control animals (broken lines) at baseline and various time points after SIV infection.

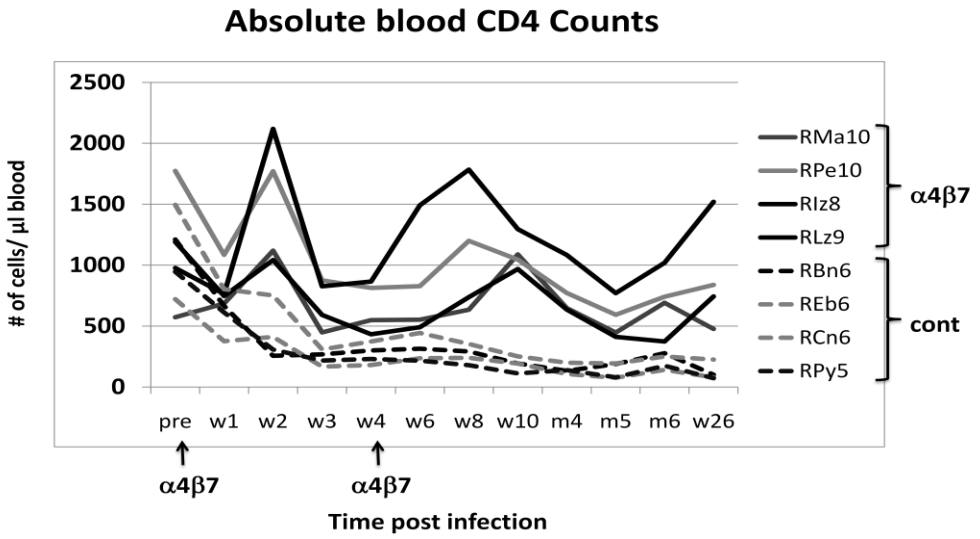

Supplemental Figure 3

Absolute numbers of CCR5- expressing $CD4^+$ T cell subsets in peripheral blood samples from the four α4β7 mAb-treated animals and the four control animals at baseline and various times after SIV infection.

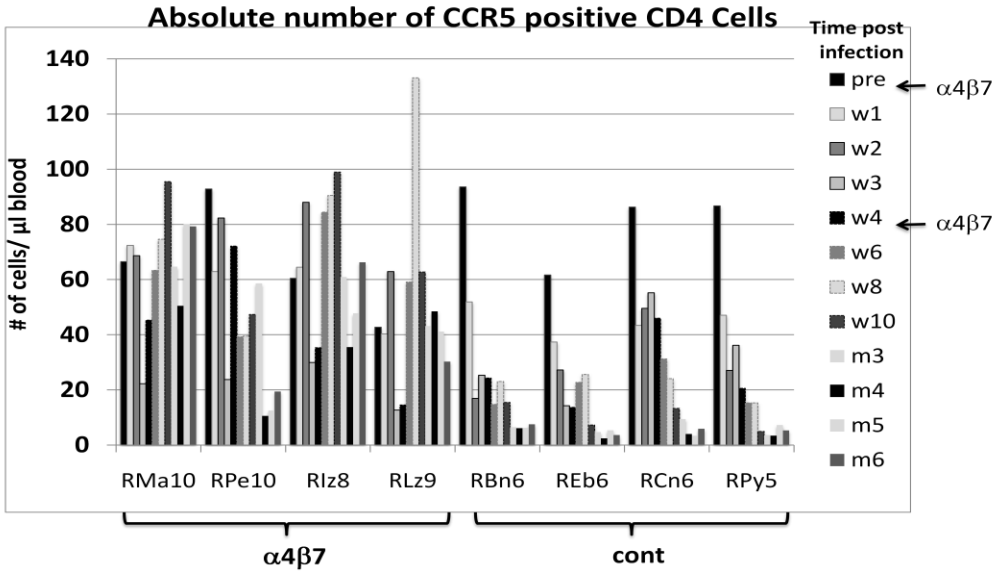

Supplemental Figure 4

Frequencies of $CD4^+$ (*top panels*) and $CD8^+$ T cells (*bottom panels*) in mononuclear cells isolated from pools of jejunal (*left panels*) and colorectal biopsies (*right panels*) from the four anti-α4β7 mAb-treated animals (solid lines) and the four control animals (broken lines) prior to (baseline) and after SIV infection.

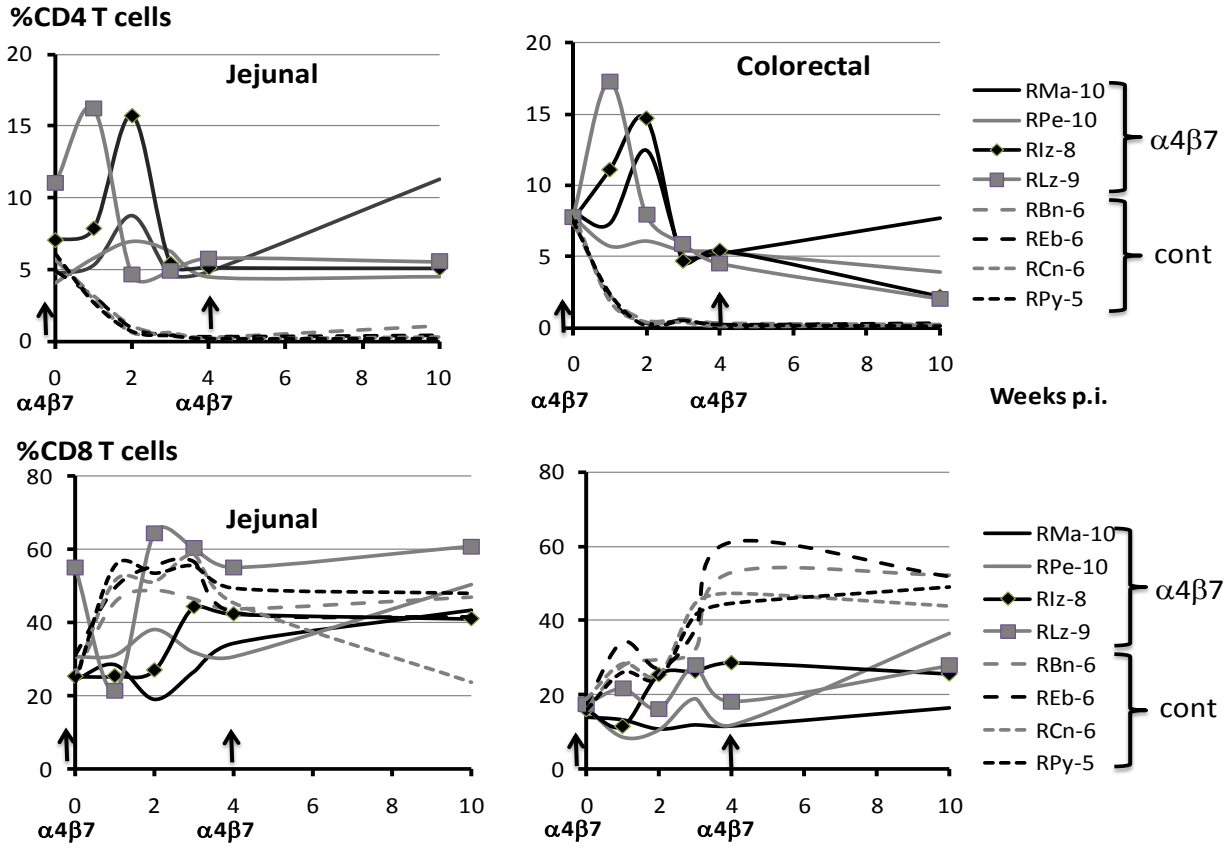

Supplemental Figure 5

Absolute numbers of the NK cells subsets in the four rhesus macaques treated with the anti-α4β7 mAb (*left panel*) and the four control animals (*right panel*). Data shown include absolute numbers of $CD3^{-}$, CD8 α/α^{+}, $NKG2a^{+}$ gated populations of (*A*) $CD16^{+}$, $CD56^{-}$ cytolytic subset and (*B*) $CD16^{-}$, $CD56^{+}$ cytokine synthesizing subset.

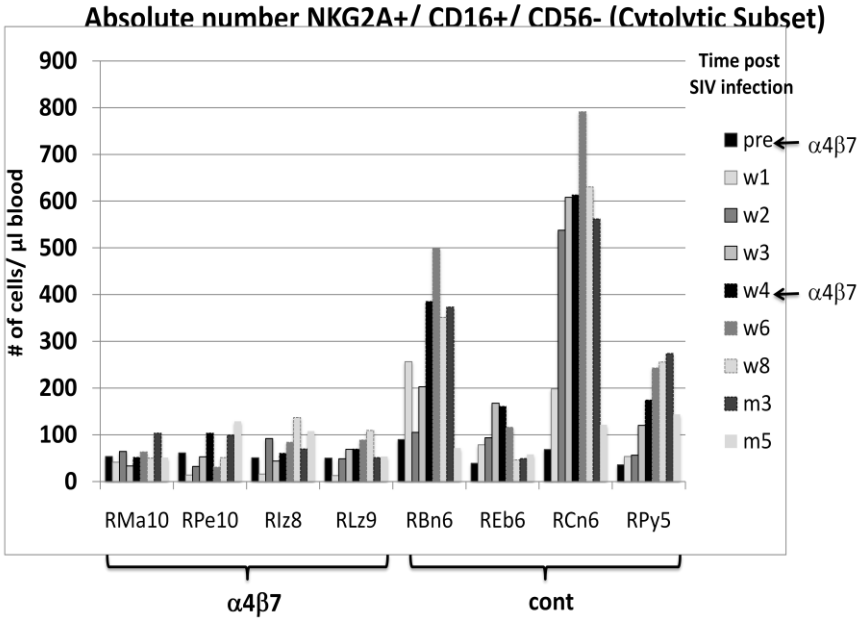

a)

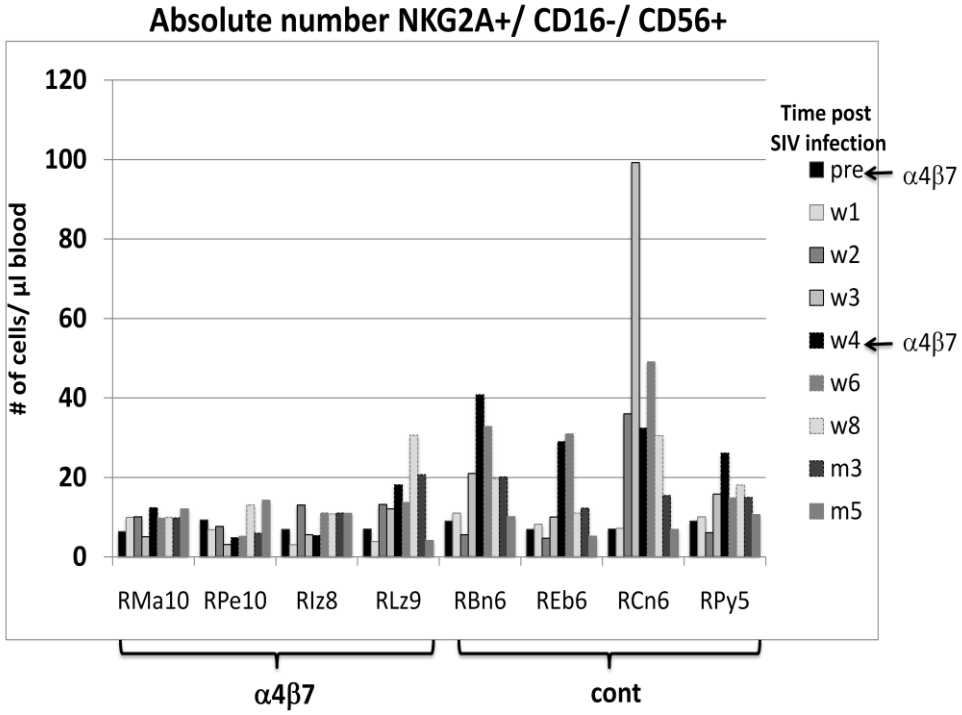

b)

Supplemental Figure 6

Effect of anti-α4β7 mAb administration on the absolute numbers of (*A*) mDCs and (*B*) pDCs prior to and after SIV infection in the four anti-α4β7 mAb-treated animals (solid lines) and the four control animals (broken lines) displayed as number of cells per microliter of blood. Note the use of different scales for values of mDCs and pDCs. The levels of pDCs at week 1 in the control animals are statistically different from the α4β7-treated animals ($p = 0.021$).

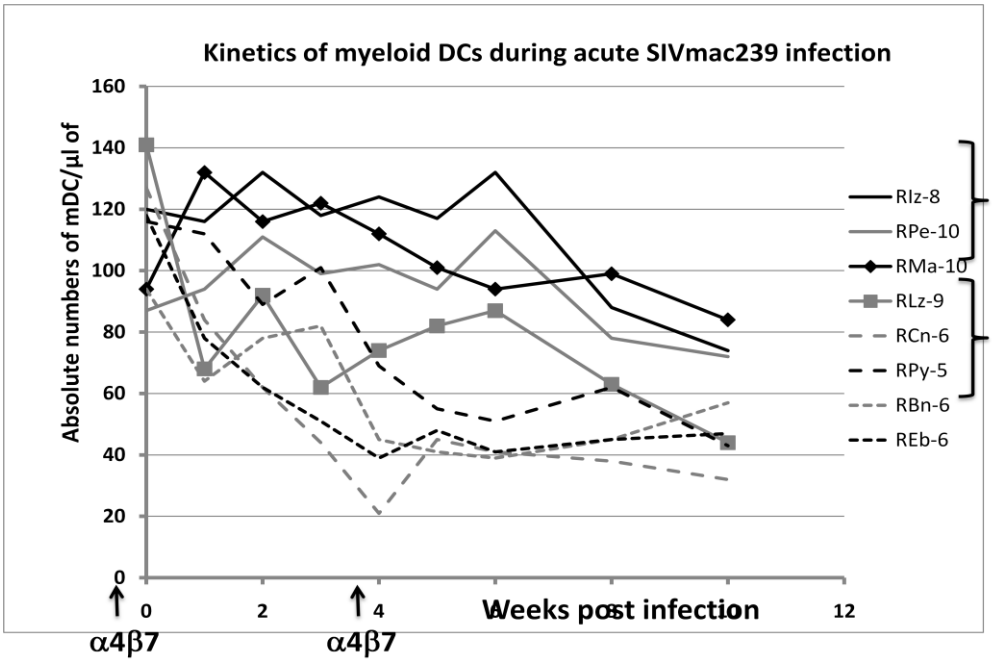

a)

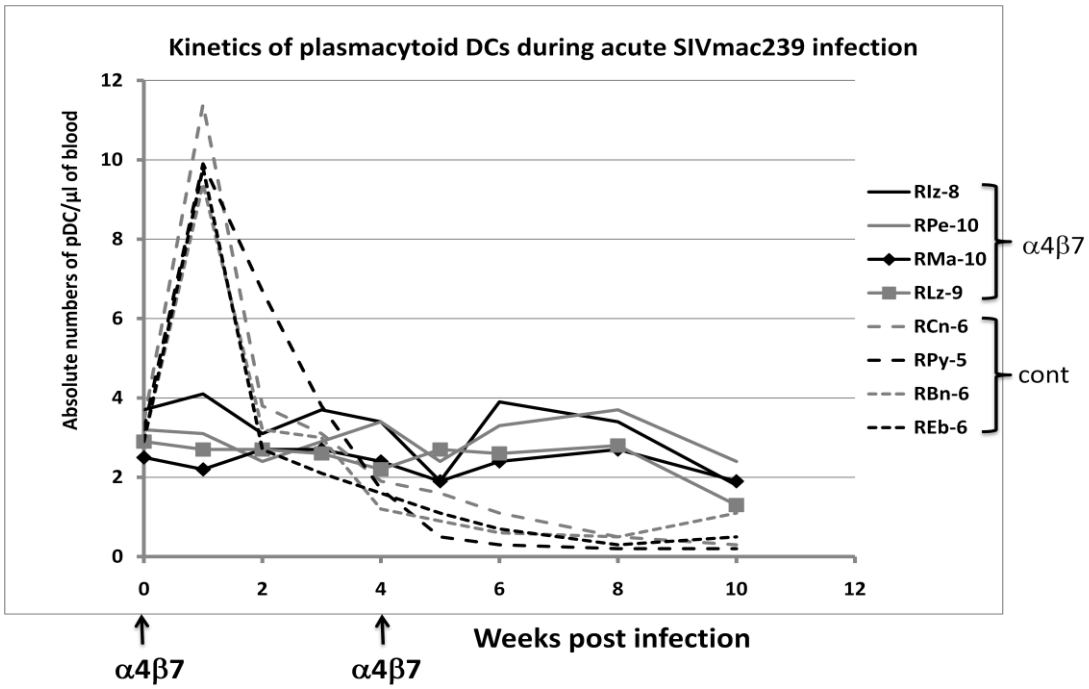

b)

References

[i] Veazey, R. S., M. DeMaria, L. V. Chalifoux, D. E. Shvetz, D. R. Pauley, H. L. Knight, M. Rosenzweig, R. P. Johnson, R. C. Desrosiers, A. A. Lackner. 1998. Gastrointestinal tract as a major site of $CD4^+$ T cell depletion and viral replication in SIV infection. Science 280: 427–431.
[ii] Brenchley, J. M., D. C. Douek. 2008. HIV infection and the gastrointestinal immune system. Mucosal Immunol. 1: 23–30.
[iii] Paiardini, M., I. Frank, I. Pandrea, C. Apetrei, G. Silvestri. 2008. Mucosal immune dysfunction in AIDS pathogenesis. AIDS Rev. 10: 36–46.
[iv] Brenchley, J. M., T. W. Schacker, L. E. Ruff, D. A. Price, J. H. Taylor, G. J. Beilman, P. L. Nguyen, A. Khoruts, M. Larson, A. T. Haase, D. C. Douek. 2004. $CD4^+$ T cell depletion during all stages of HIV disease occurs predominantly in the gastrointestinal tract. J. Exp. Med. 200: 749–759.
[v] Haase, A. T.2010. Targeting early infection to prevent HIV-1 mucosal transmission. Nature 464: 217–223.
[vi] Miller, C. J. *et al.* Propagation and dissemination of infection after vaginal transmission of simian immunodeficiency virus. J. Virol. 79, 9217–9227 (2005)
[vii] Hu, J., Gardner, M. B. & Miller, C. J. Simian immunodeficiency virus rapidly penetrates the cervicovaginal mucosa after intravaginal inoculation and infects intraepithelial dendritic cells. J. Virol. 74, 6087–6095 (2000)
[viii] Zhang, Z.-Q. *et al.* Sexual transmission and propagation of simian and human immunodeficiency viruses in two distinguishable populations of CD4+ T cells. Science 286, 1353–1357 (1999).
[ix] Reinhart, T. *et al.* Simian immunodeficiency virus burden in tissues and cellular compartments during clinical latency and AIDS. J. Infect. Dis. 176, 1198–1208 (1997).
[x] Bostik, P., Y. Takahashi, A. E. Mayne, A. A. Ansari. 2010. Innate immune natural killer cells and their role in HIV and SIV infection. HIV Therapy 4: 483–504.
[xi] McDermott, M. R., J. Bienenstock. 1979. Evidence for a common mucosal immunologic system, I: Migration of B immunoblasts into intestinal, respiratory, and genital tissues. J. Immunol. 122: 1892–1898.
[xii] Sigmundsdottir, H., E. C. Butcher. 2008. Environmental cues, dendritic cells and the programming of tissue-selective lymphocyte trafficking. Nat. Immunol. 9: 981–987.
xiii Johansson-Lindbom, B., W. W. Agace. 2007. Generation of gut-homing T cells and their localization to the small intestinal mucosa. Immunol. Rev. 215: 226–242
xiv Sigmundsdottir, H., E. C. Butcher. 2008. Environmental cues, dendritic cells and the programming of tissue-selective lymphocyte trafficking. Nat. Immunol. 9: 981–987.
xv Arthos, J., C. Cicala, E. Martinelli, K. Macleod, D. Van Ryk, D. Wei, Z. Xiao, T. D. Veenstra, T. P. Conrad, R. A. Lempicki, et al. 2008. HIV-1 envelope protein binds to and signals through integrin α4β7, the gut mucosal homing receptor for peripheral T cells. Nat. Immunol. 9: 301–309.
[xvi] Kader, M., X. Wang, M. Piatak, J. Lifson, M. Roederer, R. Veazey, J. J. Mattapallil. 2009. α4+β7hiCD4+ memory T cells harbor most Th-17 cells and are preferentially infected during acute SIV infection. Mucosal Immunol. 2: 439–449.
xvii Soler, D., T. Chapman, L.L. Yang, T. Wyant, R. Egan, and E.R. Fedyk. 2009. The binding specificity and selective antagonism of vedolizumab, an anti-alpha4beta7 integrin therapeutic antibody in development for inflammatory bowel diseases. J Pharmacol Exp Ther 330:864-875.

[xviii] Pereira, L.E., N. Onlamoon, X. Wang, R. Wang, J. Li, K.A. Reimann, F. Villinger, K. Pattanapanyasat, K. Mori, and A.A. Ansari. 2009. Preliminary in vivo efficacy studies of a recombinant rhesus anti-alpha(4)beta(7) monoclonal antibody. *Cell Immunol* 259:165-176.
[xix] Chuang YJ, Swanson R. *et al.* (2001). "Heparin enhances the specificity of antithrombin for thrombin and factor Xa independent of the reactive center loop sequence. Evidence for an exosite determinant of factor Xa specificity in heparin-activated antithrombin". *J. Biol. Chem.* 276 (18): 14961–14971.
[xx] Pabst, R., M. W. Russell, P. Brandtzaeg 2008. Tissue distribution of lymphocytes and plasma cells and the role of the gut. Trends Immunol. 29: 206–208, author reply 209–210.
[xxi] Soler, D., T. Chapman, L. L. Yang, T. Wyant, R. Egan, E. R. Fedyk. 2009. The binding specificity and selective antagonism of vedolizumab, an anti-α4β7 integrin therapeutic antibody in development for inflammatory bowel diseases. J. Pharmacol. Exp. Ther. 330: 864–875.
[xxii] Arthos, J., C. Cicala, E. Martinelli, K. Macleod, D. Van Ryk, D. Wei, Z. Xiao, T. D. Veenstra, T. P. Conrad, R. A. Lempicki, et al. 2008. HIV-1 envelope protein binds to and signals through integrin α4β7, the gut mucosal homing receptor for peripheral T cells. Nat. Immunol. 9: 301–309.
[xxiii] Corthay A. How do regulator T cells work? Scand J Immunol. 2009;70:326–336.
[xxiv] Gambineri E, Torgerson TR, Ochs HD. Immune dysregulation, polyendocrinopathy, enteropathy, and X-linked inheritance (IPEX), a syndrome of systemic autoimmunity caused by mutations of FOXP3, a critical regulator of T-cell homeostasis. Curr Opin Rheumatol. 2003;15:430–435.
[xxv] Bozdogan G, Erdem E, Demirel GY, Yildirmak Y. The role of Treg cells and FoxP3 expression in immunity of β-thalassemia major AND β-thalassemia trait patients. Pediatr Hematol Oncol. 2010 Oct;27(7):534-45.
[xxvi] Bernardes SS, Borges IK, Lima JE, Milanez Pde A, Conchon-Costa I, Felipe I, Saridakis HO, Watanabe MA. Involvement of regulatory T cells in HIV immunopathogenesis. Curr HIV Res. 2010 Jun;8(4):340-6.
[xxvii] Peter W. Hunt, Alan L. Landay, Elizabeth Sinclair, Jeffrey A. Martinson, Hiroyu Hatano, Brinda Emu, Philip J. Norris, Michael P. Busch, Jeffrey N. Martin, Cicely Brooks, Joseph M. McCune,[1] and Steven G. Deeks. A Low T Regulatory Cell Response May Contribute to Both Viral Control and Generalized Immune Activation in HIV Controllers. PLoS One. 2011; 6(1): e15924.
[xxviii] Hori S, Nomura T, Sakaguchi S. Control of regulatory T cell development by the transcription factor Foxp3. Science. 2003;299:1057–1061.
[xxix] Wang R, Kozhaya L, Mercer F, Khaitan A, Fujii H, Unutmaz D. Expression of GARP selectively identifies activated human FOXP3+ regulatory T cells. Proc Natl Acad Sci U S A. 2009 Aug 11;106(32):13439-44. Epub 2009 Jul 28.
[xxx] Weaver CT, Harrington LE, Mangan PR, Gavrieli M, Murphy KM. Th17: an effector CD4 T cell lineage with regulatory T cell ties. Immunity. 2006 Jun;24(6):677-88.
[xxxi] Brigitta Stockinger. Th17 cells: An orphan with influence. *Immunology and Cell Biology* (2007) 85, 83–84. doi:10.1038/sj.icb.7100035; published online 16 January 2007
[xxxii] Liang SC, Tan XY, Luxenberg DP, Karim R, Dunussi-Joannopoulos K, Collins M, Fouser LA. Interleukin (IL)-22 and IL-17 are coexpressed by Th17 cells and cooperatively enhance expression of antimicrobial peptides. J Exp Med. 2006 Oct 2;203(10):2271-9. Epub 2006 Sep 18.
[xxxiii] Kanwar B, Favre D, McCune JM. Th17 and regulatory T cells: implications for AIDS pathogenesis. Curr Opin HIV AIDS. 2010 Mar;5(2):151-7.
[xxxiv] Dandekar S, George MD, Bäumler AJ. Th17 cells, HIV and the gut mucosal barrier. Curr Opin HIV AIDS. 2010 Mar;5(2):173-8.

[xxxv] Salgado M, Rallón NI, Rodés B, López M, Soriano V, Benito JM. Long-term non-progressors display a greater number of Th17 cells than HIV-infected typical progressors. Clin Immunol. 2011 Mar 1.
[xxxvi] Paiardini M. Th17 cells in natural SIV hosts. Curr Opin HIV AIDS. 2010 Mar;5(2):166-72.
[xxxvii] Cecchinato V, Franchini G. Th17 cells in pathogenic simian immunodeficiency virus infection of macaques. Curr Opin HIV AIDS. 2010 Mar;5(2):141-5.
[xxxviii] Weaver CT, Hatton RD, Mangan PR, Harrington LE. IL-17 family cytokines and the expanding diversity of effector T cell lineages. Annu Rev Immunol. 2007;25:821-52.
[xxxix] Casey T. Weaver, Robin D. Hatton, Paul R. Mangan, and Laurie E. Harrington. IL-17 Family Cytokines and the Expanding Diversity of Effector T Cell Lineages. Annual Review of ImmunologyVol. 25: 821-852 (Volume publication date April 2007)
[xl] Spolski, R., Leonard, W. J. (2008) Interleukin-21: basic biology and implications for cancer and autoimmunity Annu. Rev. Immunol. 26,57-79
[xli] Iannello A, Boulassel MR, Samarani S, Tremblay C, Toma E, Routy JP, Ahmad A. IL-21 enhances NK cell functions and survival in healthy and HIV-infected patients with minimal stimulation of viral replication. J Leukoc Biol. 2010 May;87(5):857-67. Epub 2010 Jan 26.
[xlii] Yue FY, Lo C, Sakhdari A, Lee EY, Kovacs CM, Benko E, Liu J, Song H, Jones RB, Sheth P, Chege D, Kaul R, Ostrowski MA. HIV-specific IL-21 producing CD4+ T cells are induced in acute and chronic progressive HIV infection and are associated with relative viral control. J Immunol. 2010 Jul 1;185(1):498-506. Epub 2010 Jun 2.
[xliii] Williams LD, Bansal A, Sabbaj S, Heath SL, Song W, Tang J, Zajac AJ, Goepfert PA. Interleukin-21-producing HIV-1-specific CD8 T cells are preferentially seen in elite controllers. J Virol. 2011 Mar;85(5):2316-24. Epub 2010 Dec 15.
[xliv] Whittington HA, Armstrong L, Uppington KM, Millar AB. Interleukin-22: a potential immunomodulatory molecule in the lung. Am J Respir Cell Mol Biol. 2004 Aug;31(2):220-6. Epub 2004 Mar 23.
[xlv] Missé D, Yssel H, Trabattoni D, Oblet C, Lo Caputo S, Mazzotta F, Pène J, Gonzalez JP, Clerici M, Veas F. IL-22 participates in an innate anti-HIV-1 host-resistance network through acute-phase protein induction. J Immunol. 2007 Jan 1;178(1):407-15.
[xlvi] Arias JF, Nishihara R, Bala M, Ikuta K. High systemic levels of interleukin-10, interleukin-22 and C-reactive protein in Indian patients are associated with low in vitro replication of HIV-1 subtype C viruses. Retrovirology. 2010 Mar 9;7:15.
[xlvii] Ahern PP, Izcue A, Maloy KJ, Powrie F. The interleukin-23 axis in intestinal inflammation. Immunol Rev. 2008 Dec;226:147-59.
[xlviii] Monteleone I, Pallone F, Monteleone G. Interleukin-23 and Th17 cells in the control of gut inflammation. Mediators Inflamm. 2009;2009:297645. Epub 2009 May 27.
[xlix] Louis S, Dutertre CA, Vimeux L, Fery L, Henno L, Diocou S, Kahi S, Deveau C, Meyer L, Goujard C, Hosmalin A. IL-23 and IL-12p70 production by monocytes and dendritic cells in primary HIV-1 infection. J Leukoc Biol. 2010 Apr;87(4):645-53. Epub 2010 Jan 22.
[l] Dillon SM, Rogers LM, Howe R, Hostetler LA, Buhrman J, McCarter MD, Wilson CC. Human intestinal lamina propria CD1c+ dendritic cells display an activated phenotype at steady state and produce IL-23 in response to TLR7/8 stimulation. J Immunol. 2010 Jun 15;184(12):6612-21. Epub 2010 May 7.
[li] Aggarwal S, Ghilardi N, Xie MH, de Sauvage FJ, Gurney AL. Interleukin-23 promotes a distinct CD4 T cell activation state characterized by the production of interleukin-17. J Biol Chem. 2003 Jan 17;278(3):1910-4. Epub 2002 Nov 3.

[lii] Herman L, Hubert P, Caberg JH, Evrard B, Kedzia W, Boniver J, Delvenne P. MIP3 alpha stimulates the migration of Langerhans cells in models of human papillomavirus (HPV)-associated (pre)neoplastic epithelium. Cancer Immunol Immunother. 2007 Jul;56(7):1087-96. Epub 2006 Dec 5.

[liii] Fontaine J, Poudrier J, Roger M. Persistence of High Blood Levels of the Chemokines CCL2, CCL19, and CCL20 During the Course of HIV Infection. AIDS Res Hum Retroviruses. 2011 Jan 23

[liv] Choi YK, Fallert BA, Murphey-Corb MA, Reinhart TA. Simian immunodeficiency virus dramatically alters expression of homeostatic chemokines and dendritic cell markers during infection in vivo. Blood. 2003 Mar 1;101(5):1684-91. Epub 2002 Oct 24.

[lv] Blackburn SD, Wherry EJ. IL-10, T cell exhaustion and viral persistence. Trends Microbiol. 2007 Apr;15(4):143-6. Epub 2007 Mar 1.

[lvi] D.G. Brooks et al., Interleukin-10 determines viral clearance or persistence in vivo, Nat. Med. **12** (2006), pp. 1301–1309.

[lvii] M. Clerici et al., Role of interleukin-10 in T helper cell dysfunction in asymptomatic individuals infected with the human immunodeficiency virus, J. Clin. Invest. **93**(1994), pp. 768–775.

[lviii] H.D. Shin et al., Genetic restriction of HIV-1 pathogenesis to AIDS by promoter alleles of IL10, Proc. Natl. Acad. Sci. U. S. A. **97** (2000), pp. 14467–14472.

[lix] Fry TJ, Mackall CL. Interleukin-7: from bench to clinic. Blood 2002; 99: 3892–904.

[lx] Capitini CM, Chisti AA, Mackall CL. Modulating T-cell homeostasis with IL-7: preclinical and clinical studies. J Intern Med. 2009 Aug;266(2):141-53.

[lxi] Fry TJ, Moniuszko M, Creekmore S et al. IL-7 therapy dramatically alters peripheral T-cell homeostasis in normal and SIV-infected nonhuman primates. Blood 2003; 101: 2294–9.

[lxii] Vassena L, Proschan M, Fauci AS, Lusso P. Interleukin 7 reduces the levels of spontaneous apoptosis in CD4+ and CD8+ T cells from HIV-1-infected individuals. Proc Natl Acad Sci USA 2007; **104**: 2355–60.

[lxiii] Letterio JJ, Roberts AB. Regulation of immune responses by TGF-beta. Annu Rev Immunol. 1998;16:137-61.

[lxiv] Lotz M, Seth P. TGF beta and HIV infection. Ann N Y Acad Sci. 1993 Jun 23;685:501-11.

[lxv] Finter NB, Chapman S, Dowd P, Johnston JM, Manna V, Sarantis N, Sheron N, Scott G, Phua S, Tatum PB. The use of interferon-alpha in virus infections. Drugs. 1991 Nov;42(5):749-65

[lxvi] Gendelman HE, Skillman DR, Meltzer MS. Interferon alpha (IFN)-macrophage interactions in human immunodeficiency virus (HIV) infection: role of IFN in the tempo and progression of HIV disease. Int Rev Immunol. 1992;8(1):43-54

[lxvii] E. Khatissian, M.G. Tovey, M.C. Cumont, V. Monceaux, P. Lebon, L. Montagnier, B. Hurtrel and L. Chakrabarti, The relationship between the interferon alpha response and viral burden in primary SIV infection, AIDS Res. Hum. Retroviruses **12** (1996), pp. 1273–1278.